

## The *JWST* UNCOVER Treasury survey: Ultradeep NIRSpec and NIRC*am* ObserVations before the Epoch of Reionization

RACHEL BEZANSON,<sup>1</sup> IVO LABBE,<sup>2</sup> KATHERINE E. WHITAKER,<sup>3,4</sup> JOEL LEJA,<sup>5,6,7</sup> SEDONA H. PRICE,<sup>1</sup> MARIJN FRANX,<sup>8</sup>  
GABRIEL BRAMMER,<sup>4</sup> DANILO MARCHESINI,<sup>9</sup> ADI ZITRIN,<sup>10</sup> BINGJIE WANG (王冰洁),<sup>5,6,7</sup> JOHN R. WEAVER,<sup>3</sup>  
LUKAS J. FURTAK,<sup>10</sup> HAKIM ATEK,<sup>11</sup> DAN COE,<sup>12,13,14</sup> SAM E. CUTLER,<sup>3</sup> PRATIKA DAYAL,<sup>15</sup> PIETER VAN DOKKUM,<sup>16</sup>  
ROBERT FELDMANN,<sup>17</sup> NATASCHA M. FÖRSTER SCHREIBER,<sup>18</sup> SELJI FUJIMOTO,<sup>19,\*</sup> MARLA GEHA,<sup>16</sup> KARL GLAZEBROOK,<sup>2</sup>  
ANNA DE GRAAFF,<sup>20</sup> JENNY E. GREENE,<sup>21</sup> STÉPHANIE JUNEAU,<sup>22</sup> SUSAN KASSIN,<sup>12</sup> MARISKA KRIEK,<sup>8</sup> GOURAV KHULLAR,<sup>1</sup>  
MICHAEL MASEDA,<sup>23</sup> LAMIYA A. MOWLA,<sup>24</sup> ADAM MUZZIN,<sup>25</sup> THEMIYA NANAYAKKARA,<sup>2</sup> ERICA J. NELSON,<sup>26</sup>  
PASCAL A. OESCH,<sup>27,4</sup> CAMILLA PACIFICI,<sup>12</sup> RICHARD PAN,<sup>9</sup> CASEY PAPOVICH,<sup>28,29</sup> DAVID J. SETTON,<sup>1</sup>  
ALICE E. SHAPLEY,<sup>30</sup> RENSKE SMIT,<sup>31</sup> MAURO STEFANON,<sup>32,33</sup> EDWARD N. TAYLOR,<sup>2</sup> AND CHRISTINA C. WILLIAMS<sup>34,35</sup>

<sup>1</sup>*Department of Physics and Astronomy and PITT PACC, University of Pittsburgh, Pittsburgh, PA 15260, USA*

<sup>2</sup>*Centre for Astrophysics and Supercomputing, Swinburne University of Technology, Melbourne, VIC 3122, Australia*

<sup>3</sup>*Department of Astronomy, University of Massachusetts, Amherst, MA 01003, USA*

<sup>4</sup>*Cosmic Dawn Center (DAWN), Niels Bohr Institute, University of Copenhagen, Jagtvej 128, København N, DK-2200, Denmark*

<sup>5</sup>*Department of Astronomy & Astrophysics, The Pennsylvania State University, University Park, PA 16802, USA*

<sup>6</sup>*Institute for Computational & Data Sciences, The Pennsylvania State University, University Park, PA 16802, USA*

<sup>7</sup>*Institute for Gravitation and the Cosmos, The Pennsylvania State University, University Park, PA 16802, USA*

<sup>8</sup>*Leiden Observatory, Leiden University, P.O.Box 9513, NL-2300 AA Leiden, The Netherlands*

<sup>9</sup>*Department of Physics and Astronomy, Tufts University, 574 Boston Ave., Medford, MA 02155, USA*

<sup>10</sup>*Physics Department, Ben-Gurion University of the Negev, P.O. Box 653, Beer-Sheva 8410501, Israel*

<sup>11</sup>*Institut d'Astrophysique de Paris, CNRS, Sorbonne Université, 98bis Boulevard Arago, 75014, Paris, France*

<sup>12</sup>*Space Telescope Science Institute (STScI), 3700 San Martin Drive, Baltimore, MD 21218, USA*

<sup>13</sup>*Association of Universities for Research in Astronomy (AURA), Inc. for the European Space Agency (ESA)*

<sup>14</sup>*Center for Astrophysical Sciences, Department of Physics and Astronomy, The Johns Hopkins University, 3400 N Charles St. Baltimore, MD 21218, USA*

<sup>15</sup>*Kapteyn Astronomical Institute, University of Groningen, P.O. Box 800, 9700 AV Groningen, The Netherlands*

<sup>16</sup>*Department of Astronomy, Yale University, New Haven, CT 06511, USA*

<sup>17</sup>*Institute for Computational Science, University of Zurich, Winterthurerstrasse 190, CH-8006 Zurich, Switzerland*

<sup>18</sup>*Max-Planck-Institut für extraterrestrische Physik, Gießenbachstraße 1, 85748 Garching, Germany*

<sup>19</sup>*Department of Astronomy, The University of Texas at Austin, Austin, TX 78712, USA*

<sup>20</sup>*Max-Planck-Institut für Astronomie, Königstuhl 17, D-69117, Heidelberg, Germany*

<sup>21</sup>*Department of Astrophysical Sciences, 4 Ivy Lane, Princeton University, Princeton, NJ 08544, USA*

<sup>22</sup>*NSF's National Optical-Infrared Astronomy Research Laboratory, 950 N. Cherry Avenue, Tucson, AZ 85719, USA*

<sup>23</sup>*Department of Astronomy, University of Wisconsin-Madison, 475 N. Charter St., Madison, WI 53706 USA*

<sup>24</sup>*Dunlap Institute for Astronomy and Astrophysics, 50 St. George Street, Toronto, Ontario, M5S 3H4, Canada*

<sup>25</sup>*Department of Physics and Astronomy, York University, 4700 Keele Street, Toronto, Ontario, ON M3J 1P3, Canada*

<sup>26</sup>*Department for Astrophysical and Planetary Science, University of Colorado, Boulder, CO 80309, USA*

<sup>27</sup>*Department of Astronomy, University of Geneva, Chemin Pegasi 51, 1290 Versoix, Switzerland*

<sup>28</sup>*Department of Physics and Astronomy, Texas A&M University, College Station, TX, 77843-4242 USA*

<sup>29</sup>*George P. and Cynthia Woods Mitchell Institute for Fundamental Physics and Astronomy, Texas A&M University, College Station, TX, 77843-4242 USA*

<sup>30</sup>*Physics & Astronomy Department, University of California: Los Angeles, 430 Portola Plaza, Los Angeles, CA 90095, USA*

<sup>31</sup>*Astrophysics Research Institute, Liverpool John Moores University, 146 Brounlow Hill, Liverpool L3 5RF, UK*

<sup>32</sup>*Departament d'Astronomia i Astrofísica, Universitat de València, C. Dr. Moliner 50, E-46100 Burjassot, Valencia, Spain*

<sup>33</sup>*Unidad Asociada CSIC "Grupo de Astrofísica Extragaláctica y Cosmología" (Instituto de Física de Cantabria - Universitat de València)*

<sup>34</sup>*NSF's National Optical-Infrared Astronomy Research Laboratory, 950 N. Cherry Avenue, Tucson, AZ 85719, USA*

<sup>35</sup>*Steward Observatory, University of Arizona, 933 North Cherry Avenue, Tucson, AZ 85721, USA*

### ABSTRACT

In this paper we describe the survey design for the Ultradeep NIRSpec and NIRC*am* ObserVations before the Epoch of Reionization (UNCOVER) Cycle 1 *JWST* Treasury program, which executed its early imaging component in November 2022. The UNCOVER survey includes ultradeep ( $\sim 29$ – $30$ AB)

imaging of  $\sim 45$  arcmin<sup>2</sup> on and around the well-studied Abell 2744 galaxy cluster at  $z = 0.308$  and will follow-up  $\sim 500$  galaxies with extremely deep low-resolution spectroscopy with the NIRSpec/PRISM during the summer of 2023, with repeat visits in summer 2024. We describe the science goals, survey design, target selection, and planned data releases. We also present and characterize the depths of the first NIRCам imaging mosaic, highlighting previously unparalleled resolved and ultra-deep 2-4 micron imaging of known objects in the field. The UNCOVER primary NIRCам mosaic spans 28.8 arcmin<sup>2</sup> in seven filters (F115W, F150W, F200W, F277W, F356W, F410M, F444W) and 16.8 arcmin<sup>2</sup> in our NIRISS parallel (F115W, F150W, F200W, F356W, and F444W). To maximize early community use of the Treasury data set, we publicly release full reduced mosaics of public *JWST* imaging including 45 arcmin<sup>2</sup> NIRCам and 17 arcmin<sup>2</sup> NIRISS mosaics on and around the Abell 2744 cluster, including the Hubble Frontier Field primary and parallel footprints.

## 1. INTRODUCTION

A lasting legacy of the *Hubble Space Telescope* (*HST*) and *Spitzer Space Telescope* is the discovery and characterization of galaxies to  $z \sim 11$ , looking back 97% of the time to the Big Bang (e.g., Coe et al. 2013; Oesch et al. 2016). Extragalactic deep fields with Hubble imaging and grism spectroscopy to  $\sim 1.6$  microns have provided a reasonably complete census of the cosmic star formation history (e.g., Madau & Dickinson 2014; Finkelstein et al. 2015; Oesch et al. 2018; Bouwens et al. 2022b), and combined with *Spitzer* imaging, constraints on the mass functions of galaxies since  $z = 3$  (e.g., Leja et al. 2020; Duncan et al. 2014; Grazian et al. 2015; Song et al. 2016; Bhatawdekar et al. 2019; Kikuchihara et al. 2020; Furtak et al. 2021; Stefanon et al. 2021). However, despite 10,000 *HST* orbits and tens of thousands of hours of *Spitzer* observations, our picture of the Universe remains highly incomplete due to reliance on *HST*-selection (rest-frame *UV* at  $z > 4$ ). This means we were biased towards the youngest, least dusty galaxies, and had been unable to study the first galaxies at  $z \gtrsim 12$ . Understanding these first galaxies is crucial since they mark the start of the process of cosmic reionization and are the first sources of metals in the Universe (e.g., Dayal & Ferrara 2018).

The *JWST* was specifically designed to address these limitations by providing high-throughput, sensitive imaging and spectroscopy at  $1 - 5 \mu\text{m}$  with the NIRCам (Rieke et al. 2005, 2003, 2023), NIRISS (Doyon et al. 2012) and NIRSpec instruments (Jakobsen et al. 2022; Rigby et al. 2023; Böker et al. 2023). These capabilities have begun to enable us to find galaxies deep into the Dark Ages ( $z = 10 - 20$ ) (e.g., Naidu et al. 2022a; Atek et al. 2023; Finkelstein et al. 2022; Donnan et al. 2023; Harikane et al. 2023; Adams et al. 2023), to directly study the faint galaxies responsible for reionizing the universe a few hundred million years later, and

identifying dusty and quiescent galaxies to low masses to redshift  $z \sim 10$  (e.g., Carnall et al. 2022; Labbé et al. 2023; Naidu et al. 2022b; Zavala et al. 2023; Nelson et al. 2023). The intrinsically faintest galaxies can be reached with the aid of gravitational lensing. Observations with *HST* along gravitational lensing galaxy clusters (e.g., in the Hubble Frontier Fields, Lotz et al. 2017) have identified some exceptionally magnified individual objects (e.g., Zitrin et al. 2014; Kelly et al. 2015), increasing effective depths of e.g., reionization era UV luminosity functions by several magnitudes (e.g., Atek et al. 2018; Ishigaki et al. 2018; Bouwens et al. 2021; Kauffmann et al. 2022; Bouwens et al. 2022b,a). However, at the faintest ends, these studies remain besieged by systematics.

It is in this context that the Ultra-deep NIRSpec and NIRCам Observations before the Epoch of Reionization (UNCOVER) Treasury survey was designed (PIs Labbé & Bezanson, *JWST*-GO#2561). UNCOVER targets the powerful lensing cluster Abell 2744 and consists of two coordinated components executed in the same cycle. First, a deep NIRCам pre-imaging mosaic in 7 filters for  $\sim 4 - 6$  hour per band, and second ultra-deep 3 - 20 hour NIRSpec/PRISM low-resolution follow up of NIRCам-detected high-redshift galaxies - each with NIRISS or NIRCам imaging parallels. The imaging and spectroscopy leverages the gravitational lensing boost to push beyond depths achievable in blank fields. Perhaps the most exciting legacy is the potential to discover “unknown unknowns”, objects we have not yet imagined or anticipated. The advance in sensitivity, wavelength coverage, and spectral resolution (in comparison to *Spitzer* imaging) is so great that we are almost guaranteed to run into surprises. Covering ultra-deep parameter space with imaging and spectroscopy early in *JWST*’s mission helps to ensure ample time for follow up studies in future cycles.

In Figure 1 we show the full area of the UNCOVER survey (purple star) in context of other *HST* (blue circles) and *JWST* Cycle 1 extragalactic deep fields

\* Hubble Fellow

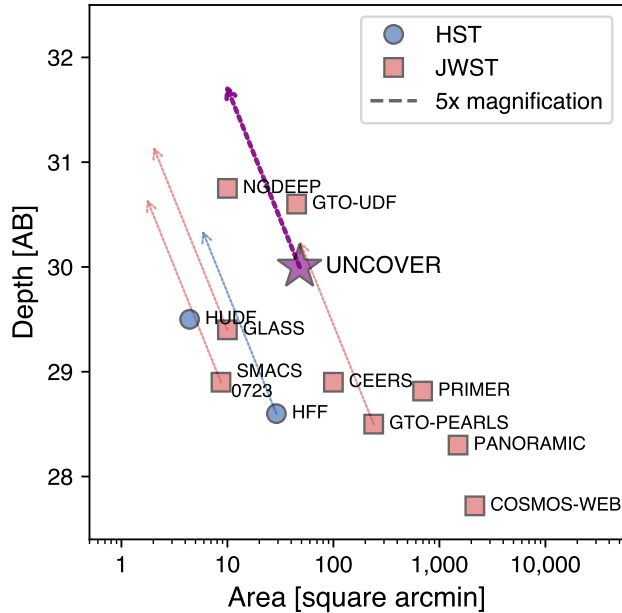


**Figure 1.** The UNCOVER combined imaging (purple star) probes a unique regime in the context of *HST* extragalactic ultra-deep fields (blue circles) and *JWST* Cycle 1 imaging surveys (red squares); without lensing it probes deeper than previous *HST* surveys and wide field programs. Gravitational lensing (approximate lensing vectors indicated by dashed arrows) from the Abell 2744 allows UNCOVER imaging to probe the intrinsically faintest objects of any *JWST* project in Cycle 1. We note that lensing vectors are approximate, as the UNCOVER survey includes lensed and unlensed areas of Abell 2744.

(red squares). UNCOVER is more than a magnitude deeper than other wide-field surveys. Only the ultra-deep NGDEEP (PIs: Finkelstein, Papovich, and Pirzkal, *JWST*-GO-2079, [Bagley et al. 2024](#)) survey and GTO ultra-deep field (JADES, PI:Eisenstein, *JWST*-GTO-1180) probe beyond UNCOVER, and these depths do not account for the effects of gravitational lensing. The Abell 2744 lensing cluster boosts the intrinsic limits of UNCOVER, sacrificing area (see arrows indicating the effect of a factor of  $\sim 5$  magnification in cluster fields) to make it the deepest extragalactic field in Cycle 1 of *JWST* observations. Furthermore, UNCOVER is the only GO dataset that collected deep spectroscopic followup of *JWST*-selected objects with no proprietary time in Cycle 1.

The outline of this paper is as follows. The survey design of the UNCOVER program is presented in §2. This paper includes the public release of early reduced mosaics of NIRC*am* cluster pre-imaging and NIRISS parallel imaging, described in §3. We summarize the science cases that will be enabled by the

UNCOVER dataset in §4. Finally, we summarize the prospects of the UNCOVER survey in §5. Throughout this paper we adopt a standard  $\Lambda$ CDM cosmology with  $H_0 = 70 \text{ km s}^{-1} \text{ Mpc}^{-1}$ ,  $\Omega_M = 0.3$ , and  $\Omega_\Lambda = 0.7$ .

## 2. SURVEY DESIGN

### 2.1. Observational Strategy

The first UNCOVER data consist of deep (4-6 hour per filter) NIRC*am* pre-imaging on the A2744 cluster to  $\sim 29.5\text{--}30\text{AB}$  magnitude in 7 filters, collected in November 2022. Nine months later July/August 2023 we targeted sources detected in NIRC*am* with ultra-deep 19 hour NIRSpec/PRISM low-resolution spectroscopy. Due to technical issues, a fraction of NIRSpec observations will be repeated in July/August 2024). Both sets of observations include deep parallel imaging (in NIRISS and NIRC*am*, respectively), to increase the area for deep photometric studies of high-redshift galaxies at mild ( $1.1\text{--}1.3\times$ ) lensing magnification. The footprints of these components are shown in Figure 2 (left panel), and reproduced along with ancillary data from *HST* and *VLT*/MUSE (center panel), as well as other Cycle 1 *JWST* data (right panel).

### 2.2. Field selection

A2744 is one of the most powerful known gravitational lensing clusters, with a large area of high magnification ( $\mu > 2, 4, 10$  over  $>17, 7, 2 \text{ arcmin}^2$ ), because the cluster itself consists of several merging subclusters, or massive subclumps (e.g., [Merten et al. 2011](#); [Richard et al. 2014](#); [Wang et al. 2015](#); [Jauzac et al. 2015](#); [Diego et al. 2016](#); [Kawamata et al. 2016](#)). The full complex stretches towards the North-West of the Hubble Frontier Field cluster pointing. The NIRC*am* footprint is designed to span the  $\mu > 2$  magnification contour (see Figure 3). The cluster contains many *HST*-detected  $6 < z < 10$  galaxies, underscoring its efficacy. The field has excellent roll angle visibility for *JWST* and low infrared background (ideal for deep background-limited observations). The observing windows (November 2022 for the imaging and expected July 2023 for spectroscopy) benefit from the lowest possible backgrounds in Cycle 1. The field also contains some of the best complementary multi-wavelength data (including deep 29AB *HST*/ACS optical data) and is accessible by the Atacama Large Millimeter/submillimeter Array (ALMA); we summarize ancillary datasets in §2.5.

### 2.3. Deep NIRC*am* and NIRISS imaging

The UNCOVER survey imaging includes deep primary NIRC*am* imaging on the extended cluster and NIRISS and NIRC*am* parallel imaging in the outskirts.

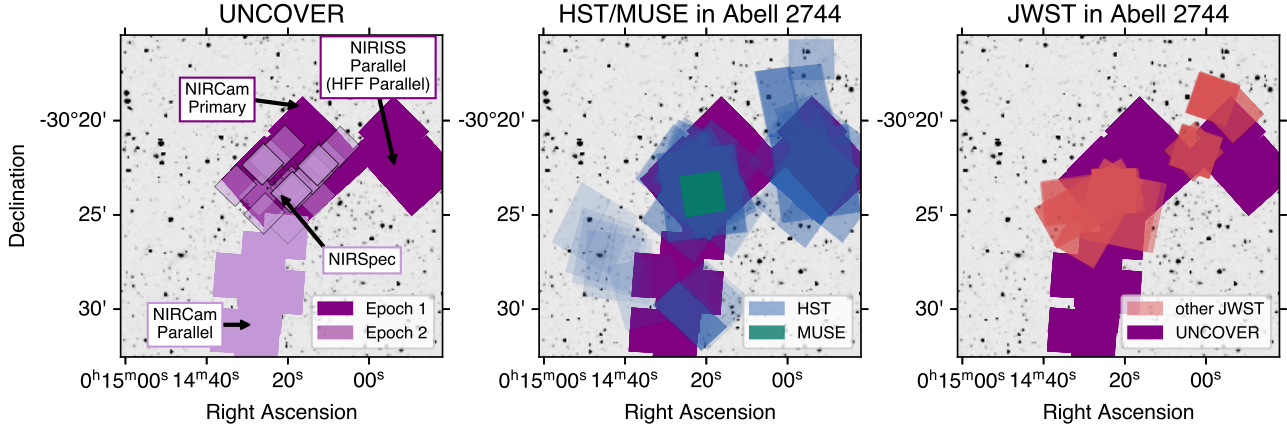


**Figure 2.** The Abell 2744 cluster has extensive deep optical/NIR (*HST* and *VLT/MUSE*) and *JWST* coverage. The *JWST*/UNCOVER footprints (purple) along with *HST* imaging (blue) and *VLT/MUSE* deep datacube (green, center) and *JWST* Cycle 1 imaging and spectroscopy (red, right) against imaging from the Legacy Imaging survey (Dey et al. 2019). An updated version with Cycle 2 *JWST* programs can be found in Suess et al. (2024). In the left panel, we highlight the detailed layout of the UNCOVER dataset, differentiating between the first epoch (dark purple, NIRCcam primary imaging and NIRISS parallel imaging) and second epoch (planned NIRSpec spectroscopy and NIRCcam parallel imaging, light purple). The NIRCcam mosaic is designed to match the  $\mu = 2$  magnification curve (see Fig.3). The footprints of the NIRSpec spectroscopy are provisional and subject to target selection.

In this section, we describe the NIRCcam primary field cluster pre-imaging mosaic and the NIRISS parallel.

The NIRCcam mosaic is designed to maximize the number of detected  $z > 10$  galaxies. This was done by forward-modeling the theoretical luminosity functions of Mason et al. (2015) and from the DELPHI model (Dayal et al. 2014, 2022) using the CATS v4.1 lens model of A2744 (Jauzac et al. 2015) to predict the number of  $6 < z < 16$  galaxies to our detection limit. The number of  $z > 10$  galaxies is maximized by a 4-pointing gap-filled NIRCcam mosaic. Our expected  $5\sigma$  depths of  $\sim 30$  AB (given  $\sim 4$  hours of exposure in F200W and  $\sim 6$  hours in F115W, *JWST* ETC 2.0, see Table 1) correspond to  $M_{UV} = -14.0$  at  $z = 6-7$  with  $< 3$  magnitudes of lensing (where models are considered more robust, e.g., Livermore et al. 2017; Atek et al. 2018; Bouwens et al. 2021). The dominant uncertainty in expected numbers is the difference between theoretical models, which can differ by factors of  $> 10$  at  $z > 10$  (e.g. Oesch et al. 2018; Finkelstein et al. 2023), with a smaller contribution from cosmic variance ranging from 10% – 40% at  $z = 7-10$  (e.g. Ucci et al. 2021). These depths compare favorably to those achieved in our final mosaic (see Table 1).

NIRCcam pre-imaging is taken with a 4-point mosaic and an 8 pointing INTRAMODULEX dither pattern for 3.7-6 hours, using six broadband filters (F115W, F150W, F200W, F277W, F356W, and F444W). A medium band filter F410M is added, to improve diagnostics of emission lines and improve photometric redshifts and stellar masses of high- $z$  galaxies (Kauffmann et al. 2020; Roberts-Borsani et al. 2021; Labbé et al.

2023). We note that the same extended mosaic was followed up with *JWST*/NIRCcam imaging as part of programs *JWST*-GO-4111 (PI Suess) and *JWST*-GO-3516 (PIs Matthee and Naidu), which added bluer broadband filters (F070W and F090W) and all remaining medium band filters. Exposure times and approximate imaging depths are listed in Table 1 and filter curves are shown in Figure 4. In that Figure, we show representative SEDs generated using *Bagpipes* (Carnall et al. 2018) with the NIRCcam primary filters. We show delayed tau models ( $\log M_{\star}/M_{\odot} = 9.2$ ) in the top four panels (100 Myr-old in purple for the earliest galaxies, and 300 Myr-old in blue for the  $z \sim 6-8$ ,  $A_V = 3$  dusty galaxies in orange, and 500-Myr-old quiescent galaxies in red). NIRISS parallel imaging includes only F115W, F150W, F200W, F356W, and F444W broad bands. This field lacks some filters with respect to the NIRCcam primary imaging as NIRISS lacks NIRCcam’s dichroic. The NIRISS parallel imaging fortuitously overlaps with 42-orbit 29AB F814W Hubble Frontier Field A2744 ACS parallel field, obviating the need for additional optical data. The first NIRCcam/ NIRISS imaging data were collected on November 2, 4, 7, and 15, 2022. The final visit was a repeat observation of visit 1:1, which initially failed guide star acquisition (on October 31, 2022). The new visit 3:1 was observed at a slightly different angle ( $V3PA = 45.00$  degrees relative to  $V3PA = 41.3588$  degrees for the other 3 visits) and higher background level to facilitate rapid rescheduling. This results in a slightly askew mosaic footprint, but image depths and footprint are minimally impacted by this change.

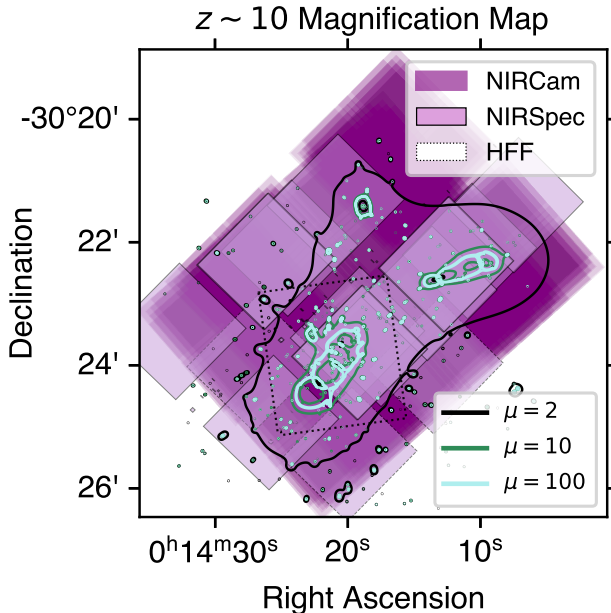


**Figure 3.** Gravitational lensing magnification contours in Abell 2744 are extremely extended, due to the complex structure of the multiple cluster cores. The above curves are taken from the UNCOVER-based lensing model at  $z \sim 10$  (Furtak et al. 2023b). The UNCOVER NIRCcam mosaic (dark purple) spans the  $\mu = 2$  curve, which is significantly larger than the Hubble Frontier Field (black dashed outline). By extending to the northern subclumps the UNCOVER mosaic enables a more detailed mapping of that region.

In parallel to the follow-up NIRSspec observations, a second imaging parallel field will be taken with NIRCcam using a more expanded set of seven broadband filters (F090W, F115W, F150W, F200W, F277W, F356W, F444W) and two medium band filters (F335M and F410M) with total exposure times of 2.6-5.3 hours. The expanded filter set mitigates the lack of optical data in that pointing. The NIRCcam parallel observations are taken with the NIRSspec/PRISM in MOS mode with a 3-POINT-WITH-NIRCcam-SIZE2 dither pattern and a three slitlet nod pattern.

#### 2.4. Scheduled NIRSspec/PRISM spectroscopic followup

The spectroscopic component of the UNCOVER survey were completed in July-August 2023, aside from a failed visit that was impacted by an electrical short. We describe the final spectroscopic program design and observational strategy in Price et al. (2024). These spectra are designed to be ultradeep, using the low-resolution ( $R \sim 30 - 300$ ) PRISM mode to provide the deepest continuum depths and widest wavelength coverage (0.6-5.3 microns). A primary goal of UN-

**Table 1.** UNCOVER Imaging

Instrument	Filter	Exposure	Dates	$5\sigma$ depth	ETC
NIRCcam (Primary)	F115W	6.0h	Nov. 2,4,7,15, 2022	30.05	29.9
	F150W	6.0h		30.18	30.1
	F200W	3.7h		30.12	30.0
	F277W	3.7h		29.75	29.5
	F356W	3.7h		29.79	29.5
	F410M	3.7h		29.03	28.8
	F444W	4.6h		29.25	29.2
NIRISS (Parallel)	F115W	3.7h	(see primary)	30.19	30.1
	F150W	3.7h		30.13	30.2
	F200W	3.7h		30.25	30.2
	F356W	2.1h		29.40	29.2
	F444W	2.1h		28.8	28.6
NIRCcam (Parallel)	F090W	5.3h	July /August 2023	—	29.7
	F115W	5.3h		—	29.8
	F150W	5.3h		—	30.0
	F200W	2.6h		—	29.8
	F277W	2.6h		—	29.3
	F335M	2.6h		—	29.0
	F356W	2.6h		—	29.3
	F410M	2.6h		—	28.6
	F444W	5.3h	—	29.2	

NOTE—Imaging depths in the NIRISS/NIRCcam mosaics are calculated using  $0.08''$  radius apertures in the short wavelength bands,  $0.16''$  radius apertures in the long wavelength bands, based on the noise properties inferred from the weight maps and corrected to total assuming point sources. The depths correspond the two-visit depth regions of the mosaic. ETC values correspond to  $S/N=5$  point source depths using JWST ETC v2.0. We refer the reader to Weaver et al. (2024) for a more detailed discussion of effective depths of our photometric catalogs and Price et al. (2024) in preparation for the NIRCcam parallel imaging.

COVER is to detect continuum flux and to measure continuum redshifts of any faint high redshift object detected securely with NIRCcam ( $10\sigma$ ,  $\sim 29AB$ ). This requires  $SNR=3$  per resolution element at  $1.5\mu m$ , which can be reached in  $\sim 20$  hours integration. For galaxies with strong emission lines, we can measure redshifts and emission line strengths to  $\sim 30AB$  if  $EW_{obs} > 600\text{\AA}$  corresponding to e.g., rest-frame  $EW_0(H\alpha, 0) > 100\text{\AA}$  at  $z=6$  or  $EW_0([OIII]_{5007}) > 60\text{\AA}$  at  $z=9$ . Typical galaxies at these redshifts have  $>5\times$  stronger emission lines (e.g., Stark 2012; Labbé et al. 2013; Smit et al. 2014; Stefanon et al. 2021, 2022; Williams et al. 2023); we expect to measure redshifts for the vast majority of targets found by NIRCcam.

The broad wavelength coverage spans critical spectral features for all potential targets. Simulated spectra for a number of targets are shown in Figure 5. From Cosmic Dawn through reionization, our PRISM spectra will

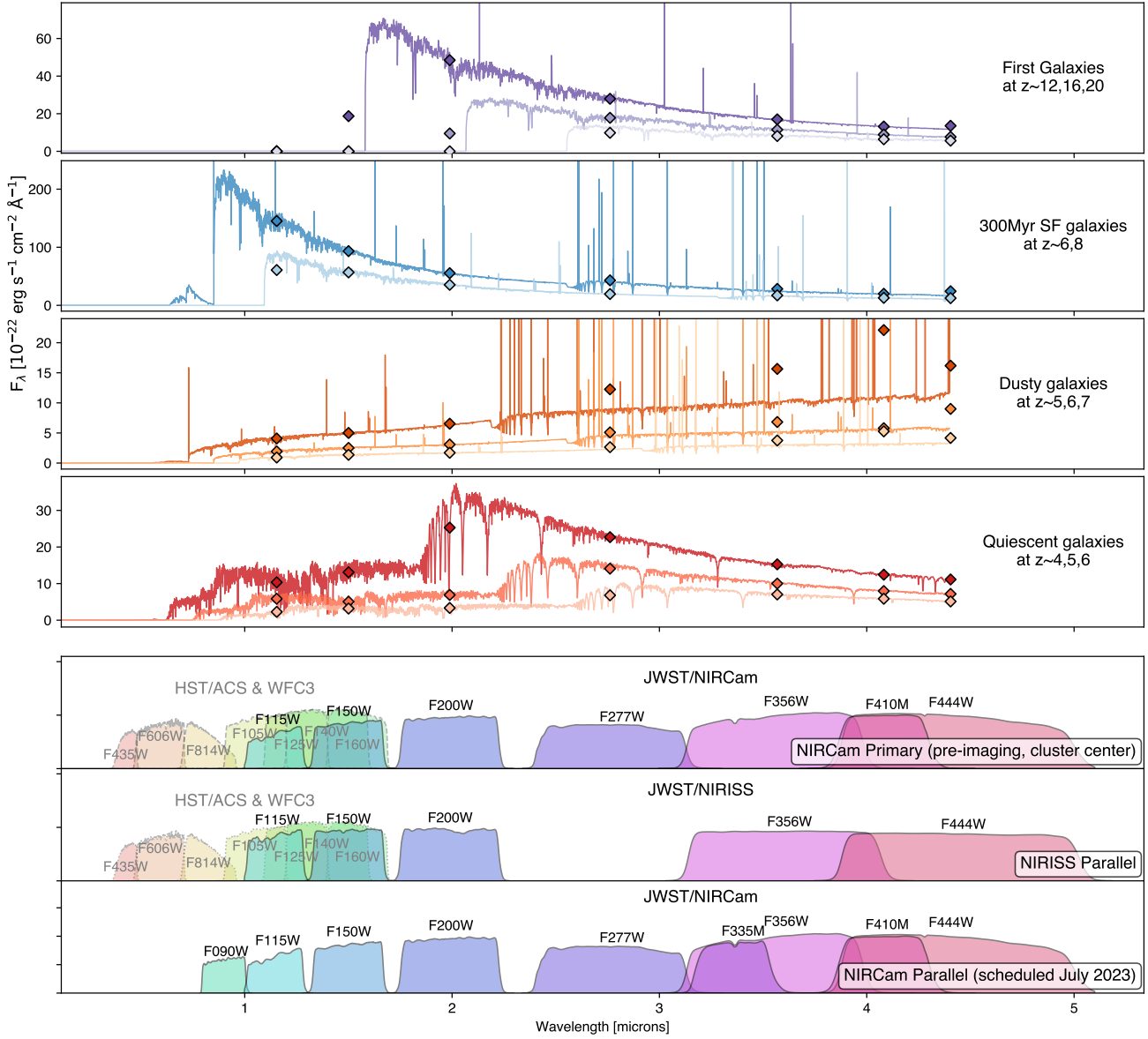


**Figure 4.** Top Rows: model SEDs for four key galaxy types and Bottom Rows: Filter curves for deep *HST* and *JWST* imaging in the 3 UNCOVER imaging fields. *HST* imaging (ACS and WFC3) from the Hubble Frontier Field (HFF) program overlaps with the Abell 2744 cluster center (UNCOVER NIRCam primary, top row) and the HFF parallel imaging overlaps with the UNCOVER NIRISS parallel (middle panel). The NIRCam parallel lacks deep optical imaging from *HST*, but includes F090W and two medium band filters (F335M and F410M).

probe UV flux and Ly $\alpha$  and will include rest-frame optical emission lines (including H $\alpha$  and [NII] below  $z \sim 7$ ). Deep exposure times probe rest-optical emission lines to measure low-level star-formation, dust attenuation, and AGN activity in dusty galaxies. Finally, the Balmer absorption features and Balmer/4000 $\text{\AA}$  breaks can be clearly detected for even the most distant quiescent candidates. We include a similar figure with real spectra in Price et al. (2024).

Our planned spectroscopic targets will be roughly prioritized according to scientific value and rarity:

- any  $z > 12$  candidates
- $z > 9$  galaxies prioritized by brightness
- Pop III candidate sources
- faint highly magnified  $6 < z < 7$  galaxies

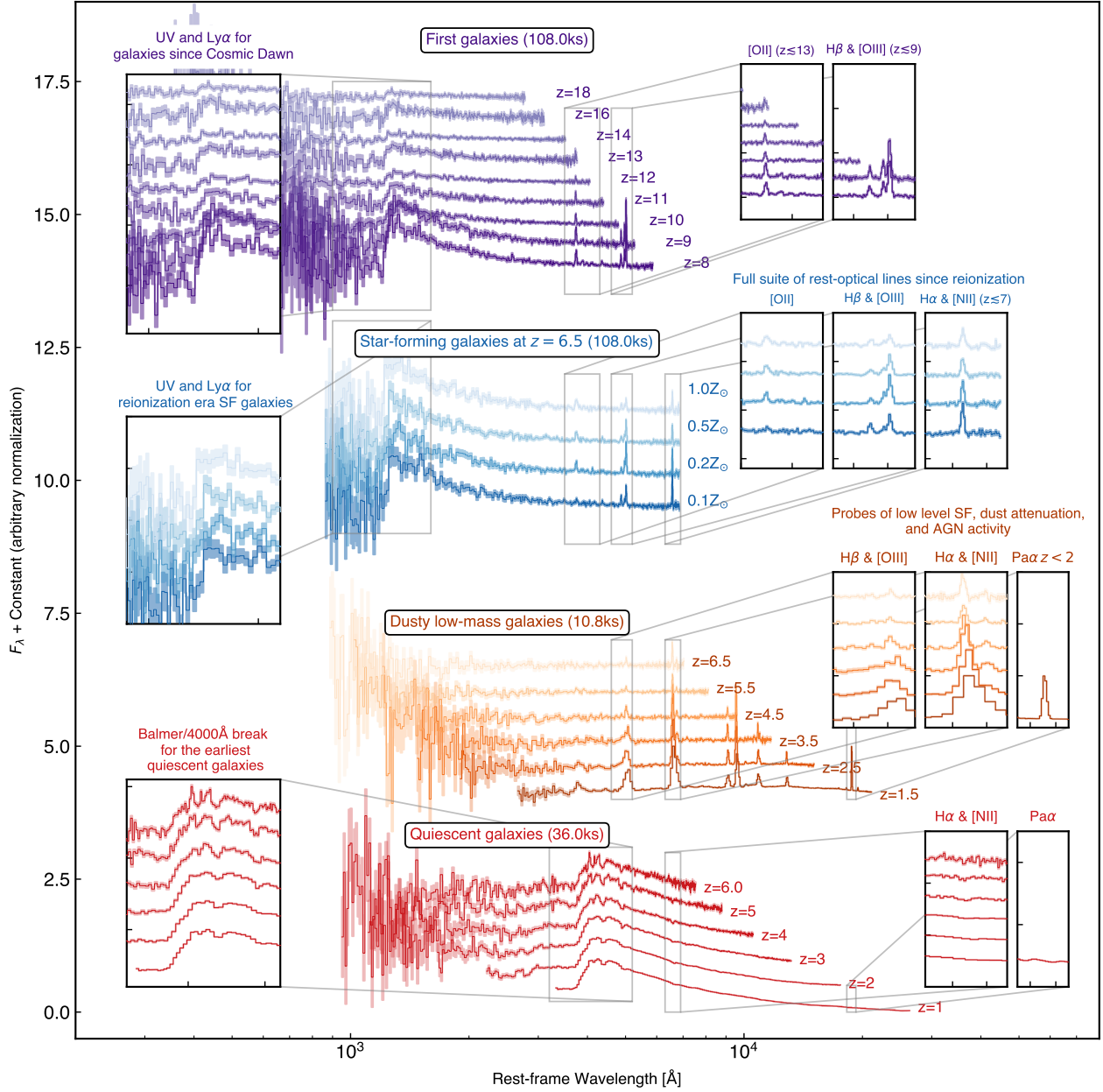


**Figure 5.** Simulated PRISM spectra of a variety of UNCOVER targets, with similar SEDs to those presented in Figure 4, with total exposure times ranging from 2.7-17.4 hours. The wide wavelength coverage (0.6-5.3 microns) of the NIRSpec/PRISM spectra catch critical spectroscopic features, with a resolution up to  $R \sim 300$  at the red end. Ultradeep exposures probe the continuum flux for nearly all sources and the multiple mask designs provide spectra for  $\sim 500 - 1000$  targets.

- quiescent galaxies  $z > 4$
- $z > 6$  AGN
- dusty galaxies  $z > 4$
- low mass quiescent galaxies at  $1 < z < 6$
- any unusual or unexpected sources
- extreme emission line galaxies
- mass-selected galaxies sampled in bins of mass and redshift

We estimate that we can accommodate  $\sim 15-20$  sources to our full depth of 17.4 hours. Other sources require less exposure time. This is accomplished by switching individual sources in and out of overlapping MSA designs (described below). Approximate numbers for key target classes are included in Table 2, estimated from Williams

**Table 2.** Predicted Galaxy Counts in UNCOVER

Category	Lensed (cluster)	Parallel
$z \gtrsim 12$ candidates	36	9
$9 < z < 12$ candidates	$\sim 100$ s	$\sim 50$
$6 \lesssim z \lesssim 7$ galaxies	$\sim 1500$	$\sim 1500$
$z > 1$ Dusty star-forming galaxies	$\sim 50$	$\sim 150$
$z > 3$ Quiescent galaxies	$> 6$	$> 10$
$1 < z < 3$ Quiescent galaxies	$> 20$	$> 60$

NOTE—The photometric dataset inevitably yielded other extraordinary targets that have been included in the MSA designs including, but not limited to: black hole seeds, extremely lensed galaxies and stars. All numbers are rough estimates derived from the JAdes extraGalactic Ultra-deep Artificial Realizations (JAGUAR) Mock Catalog (Williams et al. 2018) below  $z < 6$  and at higher redshifts from the Mason et al. (2015) model. Spectroscopic followup prioritizes highly lensed or otherwise remarkable objects.

et al. (2018) and Mason et al. (2015) models. The full implementation of this MSA design will be presented in Price et al. (2024).

The total NIRSpect integration times are designed to be split up in 7 partially overlapping dithered sequences of 2.7-4 hours each. We therefore design 7 masks with exposure time ranging from 2.7-17.4 hours, repeating the high priority objects. Each of our seven micro-shutter array (MSA) configurations are designed in an iterative manner, with the possibility of keeping objects on multiple masks. Observations will follow a 3 point dither pattern (3-POINT-WITH-NIRCAM-SIZE2). We adopt the NRSIRS2 readout pattern, averaging 5 frames into groups to optimize the noise characteristics. Given the high target density of some lower priority targets (e.g., there will be 1000s of high- $z$  emission line galaxies), we expect to fill each mask with  $\sim 100$  targets for a total of  $\sim 500$  unique sources in the spectroscopic sample.

Slit loss through the MSA will be significant and wavelength dependent due to variation in the PSF, complicating precise flux calibration. However, because the UNCOVER program includes multiband NIRCAM pre-imaging, our team is well-positioned to perform corrections for these wavelength-dependent aperture effects, leveraging flexible, spatially-resolved galaxy models (Leja et al. 2021).

### 2.5. Ancillary Datasets in Abell 2744

Abell 2744 has been targeted by a multitude of *HST* imaging, e.g., through the Hubble Frontier Fields program (Lotz et al. 2017) and the *HST*/BUFFALO sur-

vey (Steinhardt et al. 2020), which we enumerate along with a variety of other ancillary datasets in Table 3. *HST*/ACS imaging in the cluster center was taken by Program #11689 (PI: Dupke) and # 13386 (PI: Rodney) and *HST*/WFC3 observations were collected through program #13495 (PI: Lotz). In the Hubble Frontier Field parallel (UNCOVER NIRISS parallel), *HST*/ACS imaging was taken by Programs # 13386 (PI: Rodney), # 13495 (PI: Lotz), and #13389 (PI: Siana) and *HST*/WFC3 imaging in that field was taken again by the Hubble Frontier Field program (#13495, PI: Lotz). Although these deep *HST* observations were limited to the field of view of individual ACS or WFC3 pointings, the footprints were expanded by the BUFFALO survey (Program # 15117, PI: Steinhardt; Steinhardt et al. 2020), which expands the main cluster and parallel footprints by a factor of four. Recently, the deep optical coverage was expanded by Program #17231 (PI: Treu) (Paris et al. 2023). Amongst other things, this wide area enables improved lens models.

In addition, the Abell 2744 cluster has been targeted by ground-based imaging and spectroscopic programs. One such rich dataset is provided by deep *VLT*/Multi Unit Spectroscopic Explorer (MUSE) observations. This mosaic of MUSE pointings covers  $2' \times 2'$  and yields untargted spectroscopic redshifts for 514 galaxies (Mahler et al. 2018). These spectroscopic redshifts contribute to improved lensing models, especially for multiply imaged systems. Mahler et al. (2018) suggest that this improvement is approximately a factor of  $\sim 2.5$ . Although Spitzer imaging in Abell 2744 is largely superseded by novel *JWST* imaging from the UNCOVER survey, the field has also been observed in the X-ray for 110 ks by *XMM-Newton* (#074385010, PI: Kneib), 75 ks with *Suzaku* (Eckert et al. 2016), and *Chandra* (#23700107, PI Bogdan). Deep ground-based optical imaging exist from *Subaru/Suprime-Cam* in  $B$ ,  $R_C$ ,  $i'$ , and  $z'$  (Medezinski et al. 2016). ALMA observations of the Abell 2744 cluster include 1.1mm imaging of the cluster through the HFF-ALMA program (González-López et al. 2017) and a 15GHz-wide spectral scan at 1.2mm through the ALMA lensing cluster survey (ALCS) (Kohno 2019).

Already in the first cycle of *JWST* observations, several other programs targeted Abell 2744. First, the Early Release Science (ERS) GLASS-*JWST* program (Treu et al. 2022, PI: Treu) targets the cluster center with deep targeted NIRSpect spectroscopy and NIRISS imaging and untargted spectroscopy and obtains NIRCAM parallel imaging in the cluster outskirts in the following broadband filters (F090W, F115W, F150W, F200W, F277W, F356W, F444W). For details about

**Table 3.** Abell 2744 Ancillary Data

Target	Instrument	(Survey/)Program ID/PI	Notes/Depth
<b><i>JWST</i> Cycle 1</b>			
Cluster (HFF-core)	NIRSpec	GLASS/ERS-X1324/PI: Treu	52ks
	NIRISS		35ks
	NIRCam	DD-2756/PI: Chen	17ks
	NIRSpec		
	NIRCam	GTO-PEARLS/GTO-1176/PI: Windhorst	12ks
Field	NIRCam F090W, F115W, F150W, F200W F277W, F356W, F444W	GLASS/ERS-Treu/PI: Treu	30ks,50ks
<b><i>HST</i></b>			
Cluster (HFF-core)	ACS/F435W	#11689/PI:Dupke, #13386/PI: Rodney	18 orbits
	ACS/F606W		9 orbits
	ACS/F814W		41 orbits
	WFC3/F105W	#13495/PI:Lotz	24.5 orbits
	WFC3/F125W		12 orbits
	WFC3/F140W		10 orbits
WFC3/F160W	24.5 orbits		
Cluster (expanded)	ACS/F606W	BUFFALO, #15117, PI:Steinhardt	2/3 orbit
	ACS/F814W		4/3 orbit
	WFC3/F105W,F125W,F160W		2/3 orbit
Field	ACS/F435W	#13386/PI: Rodney, #13495/PI:Lotz, #13389/PI:Siana	6 orbits
	ACS/F606W		4 orbits
	ACS/F814W		14 orbits
	WFC3/F105W	#13495/PI:Lotz	24 orbits
	WFC3/F125W		12 orbits
	WFC3/F140W		10 orbits
WFC3/F160W	24 orbits		
	ACS/F606W,F775W	#17231, PI: Treu	15 orbits
<b><i>VLT</i></b>			
Cluster (HFF-core)	MUSE	Mahler et al. (2018)	3.5,4,4,5hr
<b><i>Subaru</i></b>			
Cluster (30'x30')	Suprime-Cam/ <i>B, R<sub>C</sub></i> <i>i', z'</i>	Medezinski et al. (2016)	27.58,26.83 26.31,26.03AB
<b><i>X-ray</i></b>			
Cluster	<i>XMM-Newton</i>	#074385010, 385 PI: Kneib	110ks
	<i>Suzaku</i>	#808008010,Eckert et al. (2016)	75ks
	<i>Chandra</i>	#23700107, PI: Bogdan	1028ks
<b><i>ALMA</i></b>			
Cluster	1.1mm imaging	ALMA#2013.1.00999.S, PI: Bauer	395.6s
	15GHz spectral scan	ALMA#2018.1.00035.L, PI: Kohno	95.5h
Cluster (4'x6')	30GHz spectral scan	ALMA#2022.1.00073.S, PI: Fujimoto	37.2h

that program, the reader is referred to the survey design paper (Treu et al. 2022). All data from the GLASS-*JWST* are available with no proprietary period. Additionally, Abell 2744 will be observed with NIRC*am* imaging as part of the *JWST* GTO PEARLS (Prime Extra-galactic Areas for Reionization and Lensing Science) program 1176 (PI: Windhorst), including  $\sim 2$  hour depth observations in F090W, F115W, F150W, F200W, F277W, F356W, F410M, and F444W to  $\sim 28 - 29\text{AB}$   $5-\sigma$  limiting depths (Windhorst et al. 2023). Recently, a DDT program (#2756, PI: Chen) was approved to image and spectroscopically image a lensed,  $z \sim 3.5$  supernova. That dataset includes two epochs of NIRC*am* imaging (F115W, F150W, F200W, F277W, F356W, and F444W) and NIRSpec/PRISM spectra in the cluster center. A number of subsequent *JWST* programs have been completed in Abell 2744; we refer the reader to Suess et al. (2024) for an updated accounting and similar figures. Finally  $4' \times 6'$  of the cluster center (in the footprint of the UNCOVER NIRC*am* imaging) has been mapped by the Deep UNCOVER-ALMA Legacy High- $z$  (DUALZ) Survey ALMA band 6 spectral scans (Fujimoto et al. 2023a).

### 2.6. Planned Data Release Schedule

While there is no proprietary period associated with the UNCOVER dataset, our team is committed to the regular public release of reduced and high-level data products to maximize community use of this Treasury program. This paper represents the first of several data releases of the UNCOVER survey (DR1); see full anticipated release schedule in Table 4. We subsequently provided two incremental data releases (DR1 and DR2) prior to the *JWST* Cycle 2 proposal deadline, providing the community with an early photometric catalog based on archival *HST* imaging and NIRC*am* pre-imaging in the Abell 2744 cluster (Weaver et al. 2024) in addition to a description and catalog of derived physical properties, including photometric redshifts and stellar population synthesis modeling with *Prospector* (Johnson et al. 2021) (Wang et al. 2024). Additionally, our team has published lensing maps that have been updated with new *JWST* sources (Furtak et al. 2023b), magnification estimates and uncertainties from this model are included in photometric catalogs. We introduced a third data release to incorporate the additional broad and medium band NIRC*am* imaging and NIRISS parallel fields along with all photometric data products (DR3 Suess et al. 2024). Within a year of our second epoch of data acquisition, we plan to publicly release reduced

NIRSpec/PRISM spectra (Price et al. 2024) and lensing maps that have been updated with new *JWST* spectroscopic redshifts DR4.

## 3. IMAGE REDUCTION AND MOSAICS

This paper focuses on the UNCOVER NIRC*am* and NIRISS imaging (on the Hubble Frontier Field parallel). A full description and public release of photometric and spectroscopic catalogs will be included in subsequent data releases and associated publications.

### 3.1. Image Reduction

All public *JWST* NIRC*am* and NIRISS exposures in the Abell 2744 cluster field were downloaded from the Mikulski Archive for Space Telescopes The UNCOVER datasets can be accessed through MAST at [10.17909/zn4s-0243](https://mast.stsci.edu/portal/#doc/obs/10.17909/zn4s-0243), which includes data from the UNCOVER program as well as imaging from the GLASSERS (PI: Treu) and DD-2756 (PI: Chen) programs. The data reduction pipeline Grism redshift and line analysis software for space-based spectroscopy (*Grizli*, version 1.6.0.dev99) was used to process, align, and co-add the exposures. A detailed description of the pipeline is provided in G. Brammer et al. in preparation.

We start with the MAST `rate.fits` products produced by Stage 1 of the *JWST* calibration pipeline (v1.8.4) using calibration set `rwst_0995.pmap`. We derive a correction for the “ $1/f$  noise” (Rauscher 2015) by subtracting the source-masked median image values computed along detector rows and columns. Bright cosmic rays that are not completely mitigated by the Level 1 exposure ramp fit can produce “snowball” residuals (Rigby et al. 2023). Rather than re-running the ramp fits, we identify likely snowballs as large groups of pixels with the `DQ = 4` bit set in the exposure data quality array and grow a conservative mask around them.

Before 2023 May, the flat-field reference files available in the *JWST* Calibration Reference Data System (CRDS) were determined from calibrations taken on the ground and did not accurately reflect the pixel-to-pixel structure in the in-flight NIRC*am* data. This is most important in the reddest filters where the background is brightest and therefore where any errors in the multiplicative flat-field correction are largest. We determined NIRC*am* “sky flat” reference files<sup>1</sup> from on-sky commissioning data from program COM-1063 (PI: Sunnquist) from normalized, source-masked exposures in each of the filter/detector combinations used in the UNCOVER field. The NIRC*am* long-wavelength CRDS flat-field reference files were updated in 2023

<sup>1</sup> <https://s3.amazonaws.com/grizli-v2/NircamSkyflats/flats.html>

**Table 4.** UNCOVER Data Release Schedule

Data Release	Description	Anticipated Date
DR1/DR2	Imaging Mosaics (this paper)	Dec. 2022
	Updated Gravitational Lens Model (Furtak et al. 2023b)	Dec. 2022
	First-look Photometric Catalogs (Weaver et al. 2024)	Dec. 2022
	Photo- <i>z</i> s and Stellar Populations (Wang et al. 2024)	Jan. 2023
DR3	Photometric Catalogs with MegaScience Medium Bands (Suess et al. 2024)	April 2024
DR4	Reduced PRISM Spectra (Price et al. 2024)	Aug. 2024

May (`jwtst_1084.pmap`) based on in-flight data; however, we use the custom sky flats that were computed in a uniform way for all short- and long-wavelength filter/detector combinations. We apply an additional mask to the exposure data quality arrays to ignore any pixels where the sky flat is outside of the range [0.7, 1.4], essentially removing approximately one out of four images of the same region on sky due to the dither pattern. Any masked pixels will not contribute to the mosaic and the total effective exposure time at those positions will therefore decrease. On average, 3.7% of pixels are masked for one reason or another in the longest UNCOVER exposures (837 s in F277W), of which  $\leq 2.8\%$  come from the snowball masking. After applying the flat-field calibration, we fit and subtract the additive “wisp” structure in some of the short-wavelength filter/detector combinations (Rigby et al. 2023) using wisp templates<sup>2</sup> derived from the GO-2561 UNCOVER data themselves.

The final step of the exposure-level processing is the photometric calibration, which was a rapidly-evolving topic of discussion at the time the UNCOVER data were taken in late 2022 (Boyer et al. 2022). This discussion was largely resolved with calibrations derived from in-flight data and provided by CRDS `jwtst_0989.pmap`. However, we adopt a residual relative correction of 0.94 for the F277W filter in the NIRCcam A module based on observations from the PRIMER program (GO-1837, PI:

Dunlop) where the same sources were observed in the same filter on both detectors<sup>3</sup>.

After the JWST-specific corrections to the exposures described above, the `grizli` pipeline processing is essentially identical to the procedure adopted earlier for data from the *Hubble Space Telescope* (e.g., Kokorev et al. 2022). The most important step of this processing is the image alignment, which is performed in two steps. The first computes shift translations based on the positions of sources identified in each individual exposure; these shifts tend to be small ( $\lesssim 0.1$  NIRCcam pixel) as the pointing control and small offsetting of the telescope are quite precise (Rigby et al. 2023). The absolute alignment is performed by aligning (shift and rotation) the UNCOVER F444W exposures to sources in the ground-based NOAO LegacySurvey DR9 catalog (Dey et al. 2019). We have verified that with this procedure the UNCOVER mosaic is aligned to the absolute frame defined by Gaia DR3 (Gaia Collaboration et al. 2023) at a level of 12 mas (Weaver et al. 2024). We then create a source list from the aligned F444W mosaic to which the exposures in all of the other filters are aligned. The background pedestal level of each exposure are computed with the AstroDrizzle software (Gonzaga et al. 2012), which is then also used to create the final mosaics of each filter drizzled to a common pixel grid with

<sup>3</sup> See <https://github.com/gbrammer/grizli/pull/143>

<sup>2</sup> <https://s3.amazonaws.com/grizli-v2/NircamWisp/index.html>

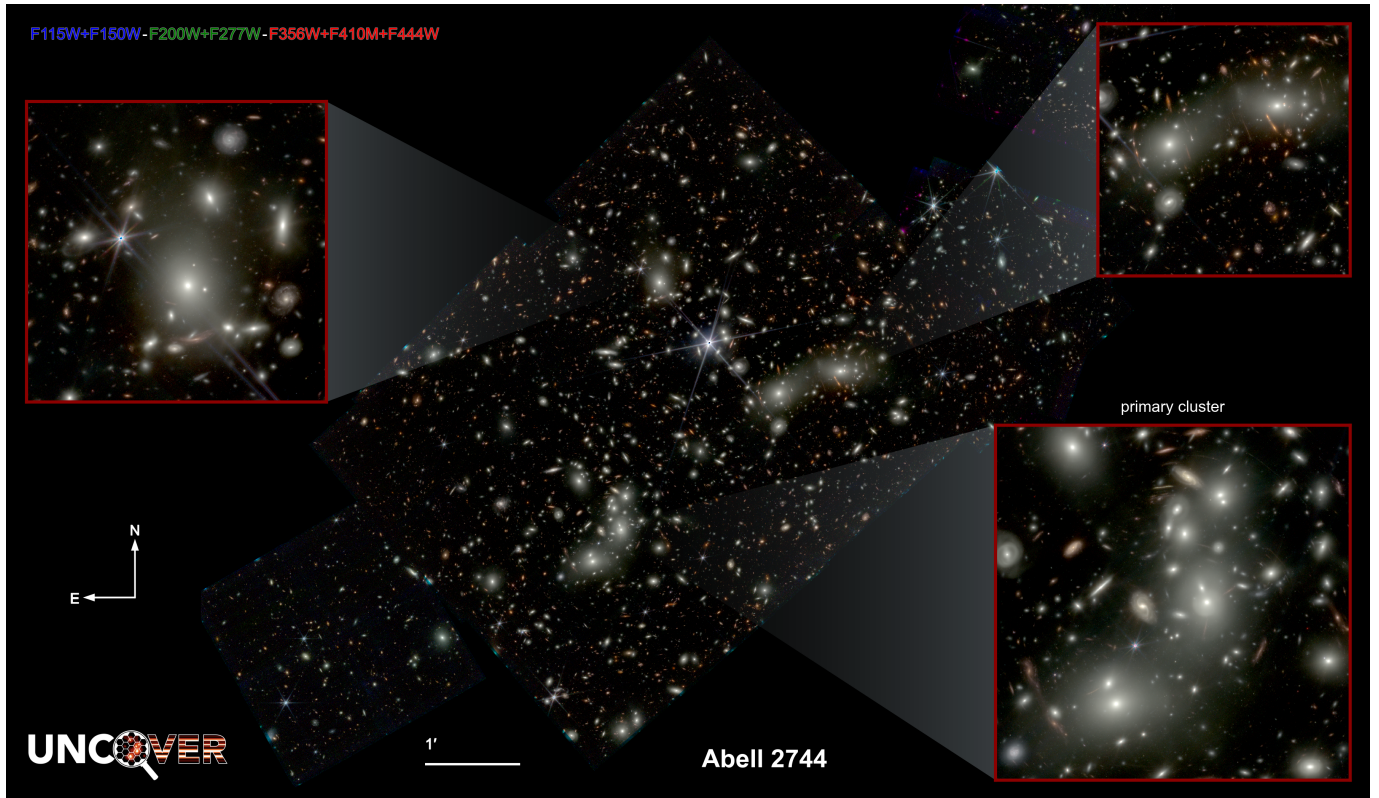


**Figure 6.** JWST imaging mosaic of Abell 2744, centered on the UNCOVER NIRC*am* mosaic. We highlight the three observed cluster cores in inset panels; only the Southern primary cluster has been covered by HST imaging in the field. Our imaging of the Northern substructures reveals a multitude of lensed features, that are used to improve the lens modeling in that region (L. Furtak et al., in preparation). This color image combines all UNCOVER filters and includes other JWST NIRC*am*/NIRISS imaging in the field including GLASS (Treu et al. 2022) and DDT#2756. High resolution version of this color image is available on the UNCOVER website.

drizzle parameters `pixfrac = 0.75`, `kernel = square`.<sup>4</sup> AstroDrizzle produces a “weight” image that has units of inverse variance of the “science” images and is made by propagating the total ERR noise model of each input exposure through the drizzle resampling. The weight map does not account for correlated noise of the finite drizzle pixel resampling (e.g., Casertano et al. 2000). We also compute mosaics of all of the historical *Hubble* imaging of the Abell 2744 field, drizzled to the same pixel grid and with datasets described by Kokorev et al. (2022) and references therein.

### 3.2. DR1: Initial Release of NIRC*am*/NIRISS Mosaics

With this publication, we publicly release fully reduced, multiband mosaics for the first NIRC*am* cluster and NIRISS parallel imaging with 20 mas pixels in NIRC*am* short-wavelengths and 40 mas pixels in the NIR-

Cam long-wavelength filters and NIRISS imaging. Color images for each mosaic are shown in Figure 6 (NIRC*am*) and Figure 7 (NIRISS). We also provide reduced *HST* imaging on the same WCS grids. All of these data products will be hosted initially through Amazon Web Services, linked from the UNCOVER team website<sup>5</sup>, and upon publication uploaded to the Barbara A. Mikulski Archive for Space Telescopes (MAST). This data release is designed to be significantly in advance of the *JWST* Cycle 2 proposal deadline. Details of this plan can be found in Table 4.

Our team intends to incrementally release higher-level data products associated with these early data (e.g., intracluster light (ICL)-subtracted mosaics, photometric catalogs and derived properties, updated gravitational lensing maps) on a short timescale. These data releases will be followed by final catalogs and spectroscopic data releases in the subsequent years.

<sup>4</sup> Note that `grizli` derives a world coordinate system (WCS) header from the JWST exposure metadata that is compatible with the Simple Imaging Polynomial convention (Shupe et al. 2005) so that the WCS from both JWST and HST exposures can be treated interchangeably.

<sup>5</sup> <https://jwst-uncover.github.io/DR1.html>

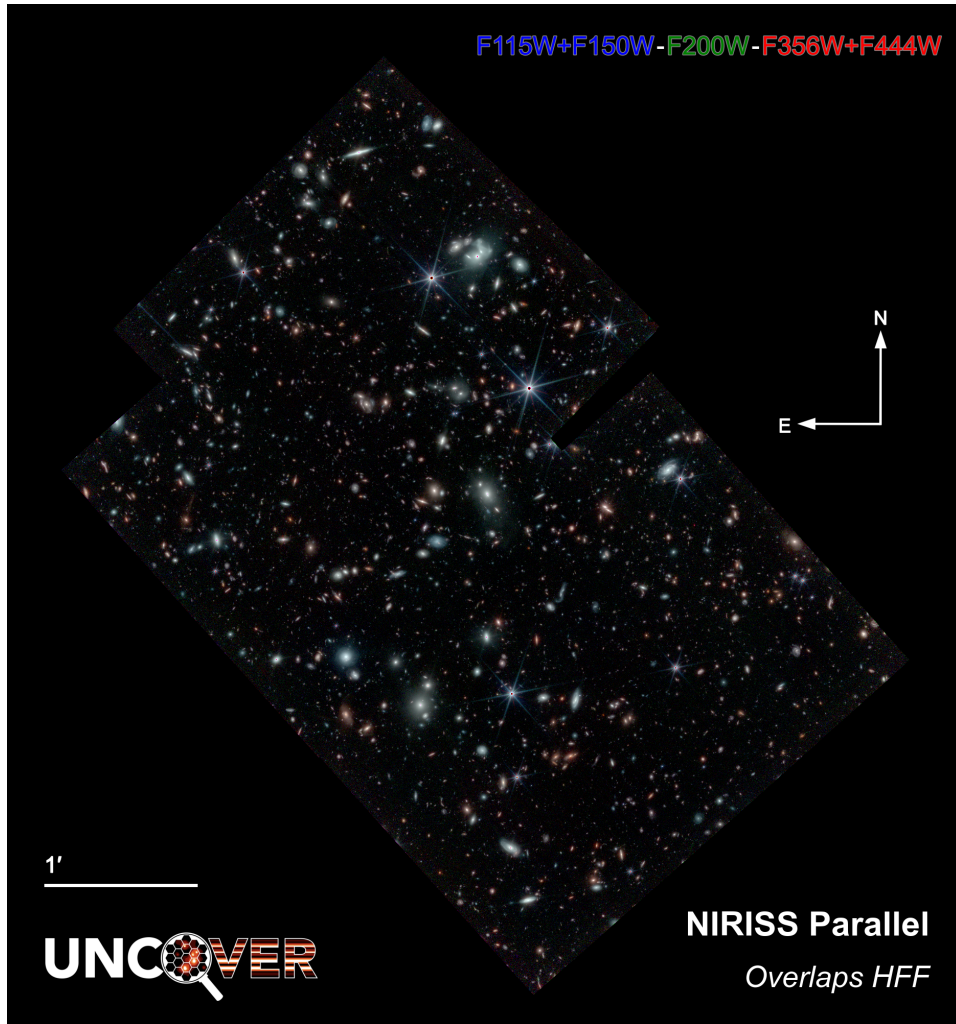


**Figure 7.** Color image of the UNCOVER NIRISS parallel, which overlaps with the Hubble Frontier field parallel.

#### 4. DISCUSSION AND SCIENTIFIC OBJECTIVES OF THE UNCOVER SURVEY

The *JWST* UNCOVER survey is designed to address a primary objective of the observatory: detecting and spectroscopically characterizing the properties of the first galaxies, while enabling a broad range of scientific explorations. Broadly, our scientific targets fall into four primary categories.

- **The First Galaxies:** The first *JWST* observations released in July 2022 quickly transformed the field. Early Release Observations in SMACSJ0723.3-7327 (ERO #2736, PI: Pontoppidan, Pontoppidan et al. 2022) and Early Release Science observations from GLASS (#1324, PI: Treu, Treu et al. 2022) and CEERS (#1345, PI: Finkelstein Bagley et al. 2023) revealed an unexpected abundance of bright galaxies at  $10 < z < 17$  (Naidu et al. 2022a; Donnan et al. 2023; Atek et al. 2023; Castellano et al. 2022; Harikane et al. 2023; Finkelstein et al. 2022;

Furtak et al. 2023a) and a population of candidate massive ( $> 10^{10} M_{\odot}$ ) galaxies at  $7 < z < 10$  (Labbé et al. 2023), which may or may not be in tension with galaxy formation model predictions (Mason et al. 2023; Ferrara et al. 2023; Boylan-Kolchin 2023; Nath et al. 2023). The NIRCам imaging from UNCOVER extends these early efforts by providing deep 3.7 hour ( $\sim 30$  AB F200W) imaging over a large area with gravitational lensing ( $\mu > 2$  over  $> 17$  arcmin<sup>2</sup>), ideally suited to improve statistics of galaxies at  $z > 10$  (see Table 2). The ultradeep 2.7 – 20 hour  $R \sim 100$  PRISM spectra can provide spectroscopic continuum redshifts of any *JWST*-selected galaxy to 29AB, unbiased with respect to the presence of emission lines or targeting, providing the first comprehensive test of the photometric selection at these redshifts. The early UNCOVER spectra revealed a number of stunning examples of these incredibly

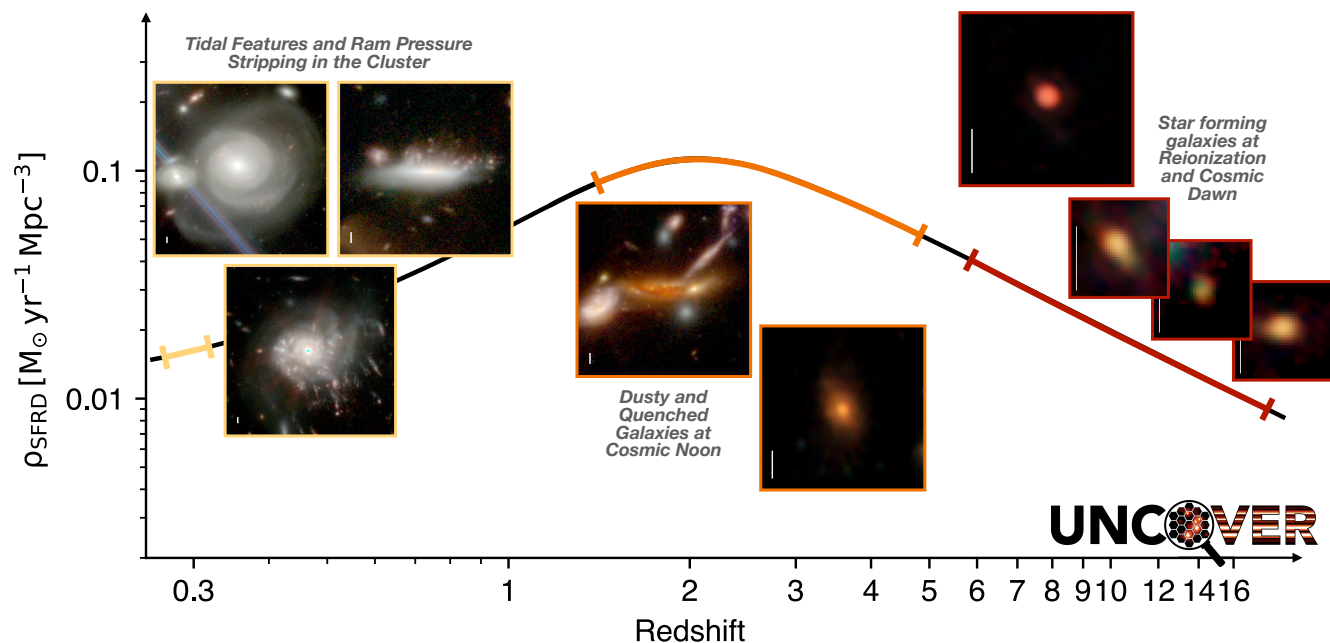


**Figure 8.** The UNCOVER imaging reveals spectacular views of a vast array of galaxies across cosmic time, shown here as drawn from the history of the cosmic star formation rate density from Casey et al. (2018). These galaxies span foreground galaxies within the Abell 2744 cluster, to red and/or remarkably resolved lensed systems at Cosmic Noon (sub-mm galaxy A2744-ID02 from González-López et al. (2017) and a quiescent galaxy candidate), and back into the most extreme – and therefore uncertain – epochs to the time of the first galaxies (GLASSz8-1 from Roberts-Borsani et al. (2022) and triply-lensed JD1 from Zitrin et al. (2014)). White scale bars indicate  $0.5''$  in all postage stamps.

distant galaxies (Wang et al. 2023; Fujimoto et al. 2023b).

- The Reionization Era: Understanding how and when galaxies irradiated their environment and reionized the surrounding neutral gas is a key outstanding question. To determine the contribution of galaxies to reionization requires a full accounting of the faintest galaxies that dominate the integrated UV light, the rate at which they produce ionizing photons, and the fraction of photons that escape. UNCOVER imaging will securely detect galaxies to  $M_{UV} \sim -14$  and should settle the issue of the potential turnover (e.g., Bouwens et al. 2022b), directly measuring 85% of the reionizing UV radiation (e.g., Livermore et al. 2017, and references therein). The  $3\times$  spatial resolution improvement of NIRCcam versus *HST*/WFC3 better constrains the size distribution of the galaxy population, further mitigating systematic sources of error. Ultra-deep PRISM spectra enables for the study of ionizing spectra of the faintest galaxies (down to  $M_{UV} \sim -15$ ) (Atek et al. 2024). Of the expected  $\sim 1500$  galaxies at  $z=6-7$ , we estimate about  $\sim 40$  will have intrinsic UV magnitudes of  $M_{UV} > -16$  but still be bright enough ( $< 28AB$ ) to

get high quality spectra. For these galaxies we will observe the full complement of strong optical lines ([OII], [OIII],  $H\beta$ ,  $H\alpha$ , [NII], [SII], with  $H\alpha$  and [NII] marginally resolved at  $R \sim 300$  at  $\sim 5\mu\text{m}$ ), to study ISM properties, ages, metallicities, and ionization mechanisms. The combination of imaging and spectra has the potential to be a quantum leap in studies of reionization era galaxies.

- The Emergence of Dusty Galaxies: The fraction of star formation missed due to dust at  $z > 4$  and at low luminosities remains unclear. ALMA has discovered dusty galaxies with relatively low masses and SFRs already at  $z > 5$  (e.g., Yamaguchi et al. 2019; Wang et al. 2019; Williams et al. 2019; Fudamoto et al. 2021; Algera et al. 2023; Dayal et al. 2022), suggesting that dust obscured star formation may be more prominent than was expected. These highly obscured extreme starbursts known to exist may represent only the tip of the iceberg. Detection of starlight from “*HST*-dark” galaxies was expected in deep JWST imaging; early imaging has indeed revealed a substantial population (Barrufet et al. 2023; Nelson et al. 2023; Pérez-González et al. 2023; Price et al. 2023) of extreme red, dusty galaxies extending to  $z \sim 7-8$ .

UNCOVER will place strong constraints at the lowest masses and the highest redshifts, complementary to the *JWST* wide-field programs (e.g., COSMOS-Web (GO #1727, PI: Kartaltepe and Casey; Casey et al. 2023), PANORAMIC (GO #2514, PI: Williams and Oesch)) capable of finding massive obscured galaxies over larger volumes. The ability to detect any highly obscured  $M_* > 10^9 M_\odot$  galaxy to  $z=9$  with NIRCcam and test photometric stellar population inferences with NIRSpec spectroscopy will further expand our census of star formation.

- **The Epoch of Quenching:** Quenching of star formation is a complex phenomenon, with different processes dominating over a range of times, mass scales, and environments. The earliest massive quiescent galaxies have been spectroscopically confirmed to redshift  $z \sim 4$  (e.g., Glazebrook et al. 2017; Schreiber et al. 2018; Forrest et al. 2020). However, this is entirely limited by detection: quiescent galaxies almost certainly exist to lower masses and higher redshift beyond the capabilities of *HST* and ground-based spectroscopy. The first *JWST* imaging has already provided spectacular candidates of massive, quiescent galaxies to redshift  $\sim 5$  (Carnall et al. 2022). UNCOVER NIRCcam imaging will extend the search for quiescent galaxies to unprecedented low mass and high redshift, i.e.,  $< 10^9 M_\odot$  to  $z=9$ . Marchesini et al. (2023) demonstrated the presence of  $10^{10} M_\odot$  quiescent galaxies to  $z \sim 2.5$  with early NIRISS spectra. The UNCOVER NIRSpec/PRISM spectroscopy will be able to push this to even lower masses and higher redshifts due to the improved depth and wavelength coverage to  $\sim 5.3$  microns to confirm the quiescence through the absence of emission lines and strong Balmer breaks (e.g., Setton et al. 2024). Beyond identification and counting, the PRISM spectroscopy will also be deep enough to further constrain stellar populations to  $F444W \lesssim 27.5$ AB from the stellar continuum.
- **The Unknown Unknowns:** Perhaps the most exciting legacy of deep fields like UNCOVER is the potential to discover objects that we have not yet imagined or identify predicted objects that we never hoped to detect in addition to offering possible constraints on the non- $\Lambda$ CDM nature of dark matter (e.g., Dayal et al. 2015). The advance in sensitivity, wavelength coverage, and spectral resolution is so large that we will certainly run into surprises. The UNCOVER treasury program en-

sures a comprehensive exploration of ultra-deep parameter space with public imaging and spectroscopy released early in *JWST*'s mission. An extraordinary example of this fruitful discovery space has been the abundance of actively accreting black holes that have been discovered and studied within the UNCOVER imaging (e.g., Furtak et al. 2023c; Greene et al. 2024) and spectroscopy (e.g., Furtak et al. 2024; Goulding et al. 2023; Kokorev et al. 2023).

The astronomical community has only begun to scratch the surface of possible *JWST* observations of the distant Universe. This paper aims to present a basic description of the UNCOVER Treasury program to optimize community use of early data products, prepare for Cycle 2 *JWST* proposals targeting objects in and behind the Abell 2744 cluster, and anticipate use of the scheduled NIRSpec/PRISM follow-up. These studies are likely to range from detailed analysis of previously known sources to exciting *JWST* discoveries. We conclude this paper by highlighting the broad range of UNCOVER scientific targets in Figure 8. Individual objects are plotted against the backdrop of dust-rich and dust-poor models for the evolution of the star formation rate density from (Casey et al. 2018).

Even in Cycle 1, the community had access to a wide range of exciting *JWST* datasets probing the distant Universe. Some of these programs will enable detailed high-resolution studies of extremely lensed sources, as in TEMPLATES (ERS # 1355, PI: Rigby and Viera). The *JWST*-GLASS program (ERS # 1324, PI: Treu) provides an in-depth and multi-pronged view of reionization in the Abell 2744 cluster (Treu et al. 2022). The CEERS program provides a range of relatively shallow imaging and spectroscopy across the well-studied CANDLES/EGS field (ERS #1324, PI: Finkelstein; Finkelstein et al. 2023). Other GO programs will expand imaging footprints: PRIMER (GO #1837, PI: Dunlop) will map nearly 700 sq. arcmin with 10 NIRCcam and MIRI filters (236 sq. arcmin in MIRI) and COSMOS-Web will map an incredible 0.6 square degrees in NIRCcam and 0.2 square degrees in MIRI with a smaller number of filters (GO #1727, PI: Kartaltepe and Casey; Casey et al. 2023). Finally, the pure parallel program PANORAMIC (GO #2514, PI: Williams and Oesch) is planned to provide multi-band NIRCcam imaging of spatially uncorrelated pointings covering up to 0.4 square degrees with a range of depths.

The UNCOVER program explores a unique parameter space; reaching within  $\sim$  a magnitude of the GTO ultradeep field but boosted by gravitational lensing and with no proprietary access. Although this is just the first

of several planned public data releases, our team looks forward to seeing what the community will uncover from this and all other *JWST* treasure troves.

RB acknowledges support from the Research Corporation for Scientific Advancement (RCSA) Cottrell Scholar Award ID No: 27587. Cloud-based data processing and file storage for this work is provided by the AWS Cloud Credits for Research program. This work is based in part on observations made with the NASA/ESA/CSA *James Webb Space Telescope*. The data were obtained from the Mikulski Archive for Space Telescopes at the Space Telescope Science Institute, which is operated by the Association of Universities for Research in Astronomy, Inc., under NASA contract NAS 5-03127 for *JWST*. These observations are associated with *JWST* Cycle 1 GO programs #2561, JWST-ERS-1324, JWST-DD-2756. Support for program JWST-GO-2561 was provided by NASA through a grant from the Space Telescope Science Institute, which is operated by the Associations of Universities for Research in Astronomy, Incorporated, under NASA contract NAS5-26555. This research is based on observations made with the NASA/ESA Hubble Space Telescope obtained from the Space Telescope Science Institute, which is operated by the Association of Universities for Research in Astronomy, Inc., under NASA contract NAS 5-26555. These observations are associated with programs HST-GO-11689, HST-GO-13386, HST-GO/DD-13495, HST-GO-13389, HST-GO-15117, and HST-GO/DD-17231. The Cosmic Dawn Center is funded by the Danish National Research Foundation (DNRF) under grant #140. This research was supported in part by the University of Pittsburgh Center for Research Computing, RRID:SCR\_022735, through the resources provided. Specifically, this work used the H2P cluster, which is supported by NSF award number OAC-2117681. LF and AZ acknowledge support by Grant No. 2020750 from the United States-Israel Binational Science Foundation (BSF) and Grant No. 2109066 from the United States National Science Foundation (NSF), and by the Ministry of Science & Technology, Israel. PD acknowledges support from the NWO grant 016.VIDI.189.162 (“ODIN”) and from the European Commission’s and University of Groningen’s CO-FUND Rosalind Franklin program. HA acknowledges support from CNES (Centre National d’Etudes Spatiales). RS acknowledges an STFC Ernest Rutherford Fellowship (ST/S004831/1). MS acknowledges support from the CIDEAGENT/2021/059 grant, from project PID2019-109592GB-I00/AEI/10.13039/501100011033 from the Spanish Ministerio de Ciencia e Innovación - Agencia Estatal de Investigación, and from Proyecto ASFAE/2022/025 del Ministerio de Ciencia y Innovación en el marco del Plan de Recuperación, Transformación y Resiliencia del Gobierno de España. The work of CCW is supported by NOIRLab, which is managed by the Association of Universities for Research in Astronomy (AURA) under a cooperative agreement with the National Science Foundation.

*Facilities:* *JWST*(NIRCam, NIRSpec, and NIRISS), *HST*(ACS and WFC3)

*Software:* astropy (Astropy Collaboration et al. 2013, 2018, 2022), Bagpipes (Carnall et al. 2018), Grizli

Brammer & Matharu 2021, Prospector (Johnson et al. 2021), DrizzlePac (Gonzaga et al. 2012)

## REFERENCES

- Adams, N. J., Conselice, C. J., Ferreira, L., et al. 2023, MNRAS, 518, 4755, doi: [10.1093/mnras/stac3347](https://doi.org/10.1093/mnras/stac3347)
- Algera, H. S. B., Inami, H., Oesch, P. A., et al. 2023, MNRAS, 518, 6142, doi: [10.1093/mnras/stac3195](https://doi.org/10.1093/mnras/stac3195)
- Astropy Collaboration, Robitaille, T. P., Tollerud, E. J., et al. 2013, A&A, 558, A33, doi: [10.1051/0004-6361/201322068](https://doi.org/10.1051/0004-6361/201322068)
- Astropy Collaboration, Price-Whelan, A. M., Sipőcz, B. M., et al. 2018, AJ, 156, 123, doi: [10.3847/1538-3881/aabc4f](https://doi.org/10.3847/1538-3881/aabc4f)
- Astropy Collaboration, Price-Whelan, A. M., Lim, P. L., et al. 2022, ApJ, 935, 167, doi: [10.3847/1538-4357/ac7c74](https://doi.org/10.3847/1538-4357/ac7c74)
- Atek, H., Richard, J., Kneib, J.-P., & Schaerer, D. 2018, MNRAS, 479, 5184, doi: [10.1093/mnras/sty1820](https://doi.org/10.1093/mnras/sty1820)
- Atek, H., Shuntov, M., Furtak, L. J., et al. 2023, MNRAS, 519, 1201, doi: [10.1093/mnras/stac3144](https://doi.org/10.1093/mnras/stac3144)
- Atek, H., Labbé, I., Furtak, L. J., et al. 2024, Nature, 626, 975, doi: [10.1038/s41586-024-07043-6](https://doi.org/10.1038/s41586-024-07043-6)
- Bagley, M. B., Finkelstein, S. L., Koekemoer, A. M., et al. 2023, ApJL, 946, L12, doi: [10.3847/2041-8213/acbb08](https://doi.org/10.3847/2041-8213/acbb08)
- Bagley, M. B., Pirzkal, N., Finkelstein, S. L., et al. 2024, ApJL, 965, L6, doi: [10.3847/2041-8213/ad2f31](https://doi.org/10.3847/2041-8213/ad2f31)
- Barrufet, L., Oesch, P. A., Weibel, A., et al. 2023, MNRAS, 522, 449, doi: [10.1093/mnras/stad947](https://doi.org/10.1093/mnras/stad947)
- Bhatawdekar, R., Conselice, C. J., Margalef-Bentabol, B., & Duncan, K. 2019, MNRAS, 486, 3805, doi: [10.1093/mnras/stz866](https://doi.org/10.1093/mnras/stz866)
- Böker, T., Beck, T. L., Birkmann, S. M., et al. 2023, PASP, 135, 038001, doi: [10.1088/1538-3873/acb846](https://doi.org/10.1088/1538-3873/acb846)
- Bouwens, R. J., Illingworth, G., Ellis, R. S., et al. 2022a, ApJ, 931, 81, doi: [10.3847/1538-4357/ac618c](https://doi.org/10.3847/1538-4357/ac618c)
- Bouwens, R. J., Illingworth, G., Ellis, R. S., Oesch, P., & Stefanon, M. 2022b, ApJ, 940, 55, doi: [10.3847/1538-4357/ac86d1](https://doi.org/10.3847/1538-4357/ac86d1)
- Bouwens, R. J., Oesch, P. A., Stefanon, M., et al. 2021, AJ, 162, 47, doi: [10.3847/1538-3881/abf83e](https://doi.org/10.3847/1538-3881/abf83e)
- Boyer, M. L., Anderson, J., Gennaro, M., et al. 2022, Research Notes of the American Astronomical Society, 6, 191, doi: [10.3847/2515-5172/ac923a](https://doi.org/10.3847/2515-5172/ac923a)
- Boylan-Kolchin, M. 2023, Nature Astronomy, 7, 731, doi: [10.1038/s41550-023-01937-7](https://doi.org/10.1038/s41550-023-01937-7)
- Brammer, G., & Matharu, J. 2021, gbrammer/grizli: Release 2021, 1.3.2, Zenodo, Zenodo, doi: [10.5281/zenodo.5012699](https://doi.org/10.5281/zenodo.5012699)
- Carnall, A. C., McLure, R. J., Dunlop, J. S., & Davé, R. 2018, MNRAS, 480, 4379, doi: [10.1093/mnras/sty2169](https://doi.org/10.1093/mnras/sty2169)
- Carnall, A. C., McLure, R. J., Dunlop, J. S., et al. 2022, ApJ, 929, 131, doi: [10.3847/1538-4357/ac5b62](https://doi.org/10.3847/1538-4357/ac5b62)
- Casertano, S., de Mello, D., Dickinson, M., et al. 2000, AJ, 120, 2747, doi: [10.1086/316851](https://doi.org/10.1086/316851)
- Casey, C. M., Zavala, J. A., Spilker, J., et al. 2018, ApJ, 862, 77, doi: [10.3847/1538-4357/aac82d](https://doi.org/10.3847/1538-4357/aac82d)
- Casey, C. M., Kartaltepe, J. S., Drakos, N. E., et al. 2023, ApJ, 954, 31, doi: [10.3847/1538-4357/acc2bc](https://doi.org/10.3847/1538-4357/acc2bc)
- Castellano, M., Fontana, A., Treu, T., et al. 2022, ApJL, 938, L15, doi: [10.3847/2041-8213/ac94d0](https://doi.org/10.3847/2041-8213/ac94d0)
- Coe, D., Zitrin, A., Carrasco, M., et al. 2013, ApJ, 762, 32, doi: [10.1088/0004-637X/762/1/32](https://doi.org/10.1088/0004-637X/762/1/32)
- Dayal, P., & Ferrara, A. 2018, PhR, 780, 1, doi: [10.1016/j.physrep.2018.10.002](https://doi.org/10.1016/j.physrep.2018.10.002)
- Dayal, P., Ferrara, A., Dunlop, J. S., & Pacucci, F. 2014, MNRAS, 445, 2545, doi: [10.1093/mnras/stu1848](https://doi.org/10.1093/mnras/stu1848)
- Dayal, P., Mesinger, A., & Pacucci, F. 2015, ApJ, 806, 67, doi: [10.1088/0004-637X/806/1/67](https://doi.org/10.1088/0004-637X/806/1/67)
- Dayal, P., Ferrara, A., Sommovigo, L., et al. 2022, MNRAS, 512, 989, doi: [10.1093/mnras/stac537](https://doi.org/10.1093/mnras/stac537)
- Dey, A., Schlegel, D. J., Lang, D., et al. 2019, AJ, 157, 168, doi: [10.3847/1538-3881/ab089d](https://doi.org/10.3847/1538-3881/ab089d)
- Diego, J. M., Broadhurst, T., Wong, J., et al. 2016, MNRAS, 459, 3447, doi: [10.1093/mnras/stw865](https://doi.org/10.1093/mnras/stw865)
- Donnan, C. T., McLeod, D. J., Dunlop, J. S., et al. 2023, MNRAS, 518, 6011, doi: [10.1093/mnras/stac3472](https://doi.org/10.1093/mnras/stac3472)
- Doyon, R., Hutchings, J. B., Beaulieu, M., et al. 2012, in Society of Photo-Optical Instrumentation Engineers (SPIE) Conference Series, Vol. 8442, Space Telescopes and Instrumentation 2012: Optical, Infrared, and Millimeter Wave, ed. M. C. Clampin, G. G. Fazio, H. A. MacEwen, & J. Oschmann, Jacobus M., 84422R, doi: [10.1117/12.926578](https://doi.org/10.1117/12.926578)
- Duncan, K., Conselice, C. J., Mortlock, A., et al. 2014, MNRAS, 444, 2960, doi: [10.1093/mnras/stu1622](https://doi.org/10.1093/mnras/stu1622)
- Eckert, D., Jauzac, M., Vazza, F., et al. 2016, MNRAS, 461, 1302, doi: [10.1093/mnras/stw1435](https://doi.org/10.1093/mnras/stw1435)
- Ferrara, A., Pallottini, A., & Dayal, P. 2023, MNRAS, 522, 3986, doi: [10.1093/mnras/stad1095](https://doi.org/10.1093/mnras/stad1095)
- Finkelstein, S. L., Ryan, Russell E., J., Papovich, C., et al. 2015, ApJ, 810, 71, doi: [10.1088/0004-637X/810/1/71](https://doi.org/10.1088/0004-637X/810/1/71)

- Finkelstein, S. L., Bagley, M. B., Haro, P. A., et al. 2022, *ApJL*, 940, L55, doi: [10.3847/2041-8213/ac966e](https://doi.org/10.3847/2041-8213/ac966e)
- Finkelstein, S. L., Bagley, M. B., Ferguson, H. C., et al. 2023, *ApJL*, 946, L13, doi: [10.3847/2041-8213/acade4](https://doi.org/10.3847/2041-8213/acade4)
- Forrest, B., Annunziatella, M., Wilson, G., et al. 2020, *ApJL*, 890, L1, doi: [10.3847/2041-8213/ab5b9f](https://doi.org/10.3847/2041-8213/ab5b9f)
- Fudamoto, Y., Oesch, P. A., Schouws, S., et al. 2021, *Nature*, 597, 489, doi: [10.1038/s41586-021-03846-z](https://doi.org/10.1038/s41586-021-03846-z)
- Fujimoto, S., Bezanson, R., Labbe, I., et al. 2023a, arXiv e-prints, arXiv:2309.07834, doi: [10.48550/arXiv.2309.07834](https://doi.org/10.48550/arXiv.2309.07834)
- Fujimoto, S., Wang, B., Weaver, J., et al. 2023b, arXiv e-prints, arXiv:2308.11609, doi: [10.48550/arXiv.2308.11609](https://doi.org/10.48550/arXiv.2308.11609)
- Furtak, L. J., Atek, H., Lehnert, M. D., Chevallard, J., & Charlot, S. 2021, *MNRAS*, 501, 1568, doi: [10.1093/mnras/staa3760](https://doi.org/10.1093/mnras/staa3760)
- Furtak, L. J., Shuntov, M., Atek, H., et al. 2023a, *MNRAS*, 519, 3064, doi: [10.1093/mnras/stac3717](https://doi.org/10.1093/mnras/stac3717)
- Furtak, L. J., Zitrin, A., Weaver, J. R., et al. 2023b, *MNRAS*, 523, 4568, doi: [10.1093/mnras/stad1627](https://doi.org/10.1093/mnras/stad1627)
- Furtak, L. J., Zitrin, A., Plat, A., et al. 2023c, *ApJ*, 952, 142, doi: [10.3847/1538-4357/acdc9d](https://doi.org/10.3847/1538-4357/acdc9d)
- Furtak, L. J., Labbé, I., Zitrin, A., et al. 2024, *Nature*, 628, 57, doi: [10.1038/s41586-024-07184-8](https://doi.org/10.1038/s41586-024-07184-8)
- Gaia Collaboration, Vallenari, A., Brown, A. G. A., et al. 2023, *A&A*, 674, A1, doi: [10.1051/0004-6361/202243940](https://doi.org/10.1051/0004-6361/202243940)
- Glazebrook, K., Schreiber, C., Labbé, I., et al. 2017, *Nature*, 544, 71, doi: [10.1038/nature21680](https://doi.org/10.1038/nature21680)
- Gonzaga, S., Hack, W., Fruchter, A., & Mack, J. 2012, *The DrizzlePac Handbook*
- González-López, J., Bauer, F. E., Romero-Cañizales, C., et al. 2017, *A&A*, 597, A41, doi: [10.1051/0004-6361/201628806](https://doi.org/10.1051/0004-6361/201628806)
- Goulding, A. D., Greene, J. E., Setton, D. J., et al. 2023, *ApJL*, 955, L24, doi: [10.3847/2041-8213/acf7c5](https://doi.org/10.3847/2041-8213/acf7c5)
- Grazian, A., Fontana, A., Santini, P., et al. 2015, *A&A*, 575, A96, doi: [10.1051/0004-6361/201424750](https://doi.org/10.1051/0004-6361/201424750)
- Greene, J. E., Labbe, I., Goulding, A. D., et al. 2024, *ApJ*, 964, 39, doi: [10.3847/1538-4357/ad1e5f](https://doi.org/10.3847/1538-4357/ad1e5f)
- Harikane, Y., Ouchi, M., Oguri, M., et al. 2023, *ApJS*, 265, 5, doi: [10.3847/1538-4365/acaaa9](https://doi.org/10.3847/1538-4365/acaaa9)
- Ishigaki, M., Kawamata, R., Ouchi, M., et al. 2018, *ApJ*, 854, 73, doi: [10.3847/1538-4357/aaa544](https://doi.org/10.3847/1538-4357/aaa544)
- Jakobsen, P., Ferruit, P., Alves de Oliveira, C., et al. 2022, *A&A*, 661, A80, doi: [10.1051/0004-6361/202142663](https://doi.org/10.1051/0004-6361/202142663)
- Jauzac, M., Richard, J., Jullo, E., et al. 2015, *MNRAS*, 452, 1437, doi: [10.1093/mnras/stv1402](https://doi.org/10.1093/mnras/stv1402)
- Johnson, B. D., Leja, J., Conroy, C., & Speagle, J. S. 2021, *ApJS*, 254, 22, doi: [10.3847/1538-4365/abef67](https://doi.org/10.3847/1538-4365/abef67)
- Kauffmann, O. B., Le Fèvre, O., Ilbert, O., et al. 2020, *A&A*, 640, A67, doi: [10.1051/0004-6361/202037450](https://doi.org/10.1051/0004-6361/202037450)
- Kauffmann, O. B., Ilbert, O., Weaver, J. R., et al. 2022, *A&A*, 667, A65, doi: [10.1051/0004-6361/202243088](https://doi.org/10.1051/0004-6361/202243088)
- Kawamata, R., Oguri, M., Ishigaki, M., Shimasaku, K., & Ouchi, M. 2016, *ApJ*, 819, 114, doi: [10.3847/0004-637X/819/2/114](https://doi.org/10.3847/0004-637X/819/2/114)
- Kelly, P. L., Rodney, S. A., Treu, T., et al. 2015, *Science*, 347, 1123, doi: [10.1126/science.aaa3350](https://doi.org/10.1126/science.aaa3350)
- Kikuchihara, S., Ouchi, M., Ono, Y., et al. 2020, *ApJ*, 893, 60, doi: [10.3847/1538-4357/ab7d8e](https://doi.org/10.3847/1538-4357/ab7d8e)
- Kohno, K. 2019, in *ALMA2019: Science Results and Cross-Facility Synergies*, 64, doi: [10.5281/zenodo.3585294](https://doi.org/10.5281/zenodo.3585294)
- Kokorev, V., Brammer, G., Fujimoto, S., et al. 2022, *ApJS*, 263, 38, doi: [10.3847/1538-4365/ac9909](https://doi.org/10.3847/1538-4365/ac9909)
- Kokorev, V., Fujimoto, S., Labbe, I., et al. 2023, *ApJL*, 957, L7, doi: [10.3847/2041-8213/ad037a](https://doi.org/10.3847/2041-8213/ad037a)
- Labbé, I., Oesch, P. A., Bouwens, R. J., et al. 2013, *ApJL*, 777, L19, doi: [10.1088/2041-8205/777/2/L19](https://doi.org/10.1088/2041-8205/777/2/L19)
- Labbé, I., van Dokkum, P., Nelson, E., et al. 2023, *Nature*, 616, 266, doi: [10.1038/s41586-023-05786-2](https://doi.org/10.1038/s41586-023-05786-2)
- Leja, J., Speagle, J. S., Johnson, B. D., et al. 2020, *ApJ*, 893, 111, doi: [10.3847/1538-4357/ab7e27](https://doi.org/10.3847/1538-4357/ab7e27)
- Leja, J., Garg, P., Johnson, B. D., et al. 2021, Preventing the Slit-Loss Catastrophe Using Flexible, Spatially Resolved Galaxy Models, JWST Proposal. Cycle 1, ID. #2354
- Livermore, R. C., Finkelstein, S. L., & Lotz, J. M. 2017, *ApJ*, 835, 113, doi: [10.3847/1538-4357/835/2/113](https://doi.org/10.3847/1538-4357/835/2/113)
- Lotz, J. M., Koekemoer, A., Coe, D., et al. 2017, *ApJ*, 837, 97, doi: [10.3847/1538-4357/837/1/97](https://doi.org/10.3847/1538-4357/837/1/97)
- Madau, P., & Dickinson, M. 2014, *ARA&A*, 52, 415, doi: [10.1146/annurev-astro-081811-125615](https://doi.org/10.1146/annurev-astro-081811-125615)
- Mahler, G., Richard, J., Clément, B., et al. 2018, *MNRAS*, 473, 663, doi: [10.1093/mnras/stx1971](https://doi.org/10.1093/mnras/stx1971)
- Marchesini, D., Brammer, G., Morishita, T., et al. 2023, *ApJL*, 942, L25, doi: [10.3847/2041-8213/acaaac](https://doi.org/10.3847/2041-8213/acaaac)
- Mason, C. A., Trenti, M., & Treu, T. 2015, *ApJ*, 813, 21, doi: [10.1088/0004-637X/813/1/21](https://doi.org/10.1088/0004-637X/813/1/21)
- . 2023, *MNRAS*, 521, 497, doi: [10.1093/mnras/stad035](https://doi.org/10.1093/mnras/stad035)
- Medezinski, E., Umetsu, K., Okabe, N., et al. 2016, *ApJ*, 817, 24, doi: [10.3847/0004-637X/817/1/24](https://doi.org/10.3847/0004-637X/817/1/24)
- Merten, J., Coe, D., Dupke, R., et al. 2011, *MNRAS*, 417, 333, doi: [10.1111/j.1365-2966.2011.19266.x](https://doi.org/10.1111/j.1365-2966.2011.19266.x)
- Naidu, R. P., Oesch, P. A., Dokkum, P. v., et al. 2022a, *ApJL*, 940, L14, doi: [10.3847/2041-8213/ac9b22](https://doi.org/10.3847/2041-8213/ac9b22)
- Naidu, R. P., Oesch, P. A., Setton, D. J., et al. 2022b, arXiv e-prints, arXiv:2208.02794, <https://arxiv.org/abs/2208.02794>

- Nath, B. B., Vasiliev, E. O., Drozdov, S. A., & Shchekinov, Y. A. 2023, *MNRAS*, 521, 662, doi: [10.1093/mnras/stad505](https://doi.org/10.1093/mnras/stad505)
- Nelson, E. J., Suess, K. A., Bezanson, R., et al. 2023, *ApJL*, 948, L18, doi: [10.3847/2041-8213/acc1e1](https://doi.org/10.3847/2041-8213/acc1e1)
- Oesch, P. A., Bouwens, R. J., Illingworth, G. D., Labbé, I., & Stefanon, M. 2018, *ApJ*, 855, 105, doi: [10.3847/1538-4357/aab03f](https://doi.org/10.3847/1538-4357/aab03f)
- Oesch, P. A., Brammer, G., van Dokkum, P. G., et al. 2016, *ApJ*, 819, 129, doi: [10.3847/0004-637X/819/2/129](https://doi.org/10.3847/0004-637X/819/2/129)
- Paris, D., Merlin, E., Fontana, A., et al. 2023, *ApJ*, 952, 20, doi: [10.3847/1538-4357/acda8a](https://doi.org/10.3847/1538-4357/acda8a)
- Pérez-González, P. G., Barro, G., Annunziatella, M., et al. 2023, *ApJL*, 946, L16, doi: [10.3847/2041-8213/acb3a5](https://doi.org/10.3847/2041-8213/acb3a5)
- Pontoppidan, K. M., Barrientes, J., Blome, C., et al. 2022, *ApJL*, 936, L14, doi: [10.3847/2041-8213/ac8a4e](https://doi.org/10.3847/2041-8213/ac8a4e)
- Price, S. H., Suess, K. A., Williams, C. C., et al. 2023, arXiv e-prints, arXiv:2310.02500, doi: [10.48550/arXiv.2310.02500](https://doi.org/10.48550/arXiv.2310.02500)
- Price, S. H., Bezanson, R., Labbe, I., et al. 2024, arXiv e-prints, arXiv:2408.03920, doi: [10.48550/arXiv.2408.03920](https://doi.org/10.48550/arXiv.2408.03920)
- Rauscher, B. J. 2015, *PASP*, 127, 1144, doi: [10.1086/684082](https://doi.org/10.1086/684082)
- Richard, J., Jauzac, M., Limousin, M., et al. 2014, *MNRAS*, 444, 268, doi: [10.1093/mnras/stu1395](https://doi.org/10.1093/mnras/stu1395)
- Rieke, M. J., Kelly, D., & Horner, S. 2005, in *Society of Photo-Optical Instrumentation Engineers (SPIE) Conference Series*, Vol. 5904, *Cryogenic Optical Systems and Instruments XI*, ed. J. B. Heaney & L. G. Burriesci, 1–8, doi: [10.1117/12.615554](https://doi.org/10.1117/12.615554)
- Rieke, M. J., Baum, S. A., Beichman, C. A., et al. 2003, in *Society of Photo-Optical Instrumentation Engineers (SPIE) Conference Series*, Vol. 4850, *IR Space Telescopes and Instruments*, ed. J. C. Mather, 478–485, doi: [10.1117/12.489103](https://doi.org/10.1117/12.489103)
- Rieke, M. J., Kelly, D. M., Misselt, K., et al. 2023, *PASP*, 135, 028001, doi: [10.1088/1538-3873/acac53](https://doi.org/10.1088/1538-3873/acac53)
- Rigby, J., Perrin, M., McElwain, M., et al. 2023, *PASP*, 135, 048001, doi: [10.1088/1538-3873/acb293](https://doi.org/10.1088/1538-3873/acb293)
- Roberts-Borsani, G., Treu, T., Mason, C., et al. 2021, *ApJ*, 910, 86, doi: [10.3847/1538-4357/abe45b](https://doi.org/10.3847/1538-4357/abe45b)
- Roberts-Borsani, G., Morishita, T., Treu, T., et al. 2022, *ApJL*, 938, L13, doi: [10.3847/2041-8213/ac8e6e](https://doi.org/10.3847/2041-8213/ac8e6e)
- Schreiber, C., Glazebrook, K., Nanayakkara, T., et al. 2018, *A&A*, 618, A85, doi: [10.1051/0004-6361/201833070](https://doi.org/10.1051/0004-6361/201833070)
- Setton, D. J., Khullar, G., Miller, T. B., et al. 2024, arXiv e-prints, arXiv:2402.05664, doi: [10.48550/arXiv.2402.05664](https://doi.org/10.48550/arXiv.2402.05664)
- Shupe, D. L., Moshir, M., Li, J., et al. 2005, in *Astronomical Society of the Pacific Conference Series*, Vol. 347, *Astronomical Data Analysis Software and Systems XIV*, ed. P. Shopbell, M. Britton, & R. Ebert, 491
- Smit, R., Bouwens, R. J., Labbé, I., et al. 2014, *ApJ*, 784, 58, doi: [10.1088/0004-637X/784/1/58](https://doi.org/10.1088/0004-637X/784/1/58)
- Song, M., Finkelstein, S. L., Ashby, M. L. N., et al. 2016, *ApJ*, 825, 5, doi: [10.3847/0004-637X/825/1/5](https://doi.org/10.3847/0004-637X/825/1/5)
- Stark, D. 2012, *Nature*, 489, 370, doi: [10.1038/489370a](https://doi.org/10.1038/489370a)
- Stefanon, M., Bouwens, R. J., Illingworth, G. D., et al. 2022, *ApJ*, 935, 94, doi: [10.3847/1538-4357/ac7e44](https://doi.org/10.3847/1538-4357/ac7e44)
- Stefanon, M., Bouwens, R. J., Labbé, I., et al. 2021, *ApJ*, 922, 29, doi: [10.3847/1538-4357/ac1bb6](https://doi.org/10.3847/1538-4357/ac1bb6)
- Steinhardt, C. L., Jauzac, M., Acebron, A., et al. 2020, *ApJS*, 247, 64, doi: [10.3847/1538-4365/ab75ed](https://doi.org/10.3847/1538-4365/ab75ed)
- Suess, K. A., Weaver, J. R., Price, S. H., et al. 2024, arXiv e-prints, arXiv:2404.13132, doi: [10.48550/arXiv.2404.13132](https://doi.org/10.48550/arXiv.2404.13132)
- Treu, T., Roberts-Borsani, G., Bradac, M., et al. 2022, *ApJ*, 935, 110, doi: [10.3847/1538-4357/ac8158](https://doi.org/10.3847/1538-4357/ac8158)
- Ucci, G., Dayal, P., Hutter, A., et al. 2021, *Astraeus - II. Quantifying the impact of cosmic variance during the Epoch of Reionization*, *Monthly Notices of the Royal Astronomical Society*, Volume 506, Issue 1, pp.202-214, doi: [10.1093/mnras/stab1229](https://doi.org/10.1093/mnras/stab1229)
- Wang, B., Fujimoto, S., Labbé, I., et al. 2023, *ApJL*, 957, L34, doi: [10.3847/2041-8213/acfe07](https://doi.org/10.3847/2041-8213/acfe07)
- Wang, B., Leja, J., Labbé, I., et al. 2024, *ApJS*, 270, 12, doi: [10.3847/1538-4365/ad0846](https://doi.org/10.3847/1538-4365/ad0846)
- Wang, T., Schreiber, C., Elbaz, D., et al. 2019, *Nature*, 572, 211, doi: [10.1038/s41586-019-1452-4](https://doi.org/10.1038/s41586-019-1452-4)
- Wang, X., Hoag, A., Huang, K. H., et al. 2015, *ApJ*, 811, 29, doi: [10.1088/0004-637X/811/1/29](https://doi.org/10.1088/0004-637X/811/1/29)
- Weaver, J. R., Cutler, S. E., Pan, R., et al. 2024, *ApJS*, 270, 7, doi: [10.3847/1538-4365/ad07e0](https://doi.org/10.3847/1538-4365/ad07e0)
- Williams, C. C., Curtis-Lake, E., Hainline, K. N., et al. 2018, *ApJS*, 236, 33, doi: [10.3847/1538-4365/aabcbb](https://doi.org/10.3847/1538-4365/aabcbb)
- Williams, C. C., Labbe, I., Spilker, J., et al. 2019, *ApJ*, 884, 154, doi: [10.3847/1538-4357/ab44aa](https://doi.org/10.3847/1538-4357/ab44aa)
- Williams, H., Kelly, P. L., Chen, W., et al. 2023, *Science*, 380, 416, doi: [10.1126/science.adf5307](https://doi.org/10.1126/science.adf5307)
- Windhorst, R. A., Cohen, S. H., Jansen, R. A., et al. 2023, *AJ*, 165, 13, doi: [10.3847/1538-3881/aca163](https://doi.org/10.3847/1538-3881/aca163)
- Yamaguchi, Y., Kohno, K., Hatsukade, B., et al. 2019, *ApJ*, 878, 73, doi: [10.3847/1538-4357/ab0d22](https://doi.org/10.3847/1538-4357/ab0d22)
- Zavala, J. A., Buat, V., Casey, C. M., et al. 2023, *ApJL*, 943, L9, doi: [10.3847/2041-8213/acacfe](https://doi.org/10.3847/2041-8213/acacfe)
- Zitrin, A., Zheng, W., Broadhurst, T., et al. 2014, *ApJL*, 793, L12, doi: [10.1088/2041-8205/793/1/L12](https://doi.org/10.1088/2041-8205/793/1/L12)